

JOURNAL ARTICLE

A Physiologically Based Pharmacokinetic Model for the Oxime  
TMB-4: Simulation of Rodent and Human Data

13 January 2013

Teresa R. Sterner<sup>1</sup>, Christopher D. Ruark<sup>1</sup>, Tammie R. Covington<sup>1</sup>,  
Kyung O. Yu<sup>2</sup>, Jeffery M. Gearhart<sup>1</sup>

<sup>1</sup>Henry M. Jackson Foundation  
For the Advancement of Military Medicine  
<sup>2</sup>711 HPW/RHDJ, WPAFB OH

# REPORT DOCUMENTATION PAGE

Form Approved  
OMB No. 0704-0188

Public reporting burden for this collection of information is estimated to average 1 hour per response, including the time for reviewing instructions, searching existing data sources, gathering and maintaining the data needed, and completing and reviewing this collection of information. Send comments regarding this burden estimate or any other aspect of this collection of information, including suggestions for reducing this burden to Department of Defense, Washington Headquarters Services, Directorate for Information Operations and Reports (0704-0188), 1215 Jefferson Davis Highway, Suite 1204, Arlington, VA 22202-4302. Respondents should be aware that notwithstanding any other provision of law, no person shall be subject to any penalty for failing to comply with a collection of information if it does not display a currently valid OMB control number. PLEASE DO NOT RETURN YOUR FORM TO THE ABOVE ADDRESS.

<b>1. REPORT DATE (DD-MM-YYYY)</b> 13-01-13		<b>2. REPORT TYPE</b> JA		<b>3. DATES COVERED (From - To)</b> 1 Jul 2011 to 30 Nov 2011	
<b>4. TITLE AND SUBTITLE</b> A physiologically based pharmacokinetic model for the oxime TMB-4: simulation of rodent and human data				<b>5a. CONTRACT NUMBER</b>	
				<b>5b. GRANT NUMBER</b> NA	
				<b>5c. PROGRAM ELEMENT NUMBER</b> 62202F	
<b>6. AUTHOR(S)</b> Stern, Teresa R. <sup>1</sup> ; Ruark, Christopher D. <sup>1</sup> ; Covington, Tammie R.; Yu, Kyung O.*; Gearhart, Jeffery M. <sup>1</sup>				<b>5d. PROJECT NUMBER</b> ODT	
				<b>5e. TASK NUMBER</b> WP	
				<b>5f. WORK UNIT NUMBER</b> ODTWP004	
<b>7. PERFORMING ORGANIZATION NAME(S) AND ADDRESS(ES)</b> <sup>1</sup> HJF 711 HPW/RHDJ, Bldg 837 2729 R Street Wright-Patterson AFB OH 45433-5707				<b>8. PERFORMING ORGANIZATION REPORT NUMBER</b>  AFRL-RH-WP-JA-2012-0053	
<b>9. SPONSORING/MONITORING AGENCY NAME(S) AND ADDRESS(ES)</b> *Air Force Materiel Command Air Force Research Laboratory 711th Human Performance Wing Human Effectiveness Directorate Bioeffects Division Molecular Bioeffects Branch Wright-Patterson AFB OH 45433-5707				<b>10. SPONSOR/MONITOR'S ACRONYM(S)</b> 711 HPW/RHDJ	
				<b>11. SPONSORING/MONITORING AGENCY REPORT NUMBER</b>	
<b>12. DISTRIBUTION AVAILABILITY STATEMENT</b> Distribution A. Approved for public release; distribution unlimited.					
<b>13. SUPPLEMENTARY NOTES</b> Cleared 9 Aug 2012, 88ABW-2012-4052; SAF/PA 2012-0473					
<b>14. ABSTRACT</b> Multiple oximes have been synthesized and evaluated for use as countermeasures against chemical warfare nerve agents. The current U.S. military and civilian oxime countermeasure, 2-[(hydroxyimino)methyl]-1-methylpyridin-1-ium chloride (2-PAM), is under consideration for replacement with a more effective acetylcholinesterase reactivator, 1,1'-methylenebis[4-hydroxyiminomethyl]pyridinium dimethanesulfonate (MMB-4). Kinetic data in the scientific literature for MMB-4 are limited; therefore, a physiologically based pharmacokinetic (PBPK) model was developed for a structurally related oxime, 1,1'-trimethylenebis[4-hydroxyiminomethyl]pyridinium dibromide. Based on a previous model structure for the organophosphate diisopropylfluorophosphate, the model includes key sites of acetylcholinesterase inhibition (brain and diaphragm), as well as fat, kidney, liver, rapidly perfused tissues and slowly perfused tissues. All tissue compartments are diffusion limited. Model parameters were collected from the literature, predicted using quantitative structure-property relationships or, when necessary, fit to available pharmacokinetic data from the literature. The model was parameterized using rat plasma, tissue and urine time course data from intramuscular administration, as well as human blood and urine data from intravenous and intramuscular administration; sensitivity analyses were performed. The PBPK model successfully simulates rat and human data sets and has been evaluated by predicting intravenous mouse and intramuscular human data not used in the development of the model. Monte Carlo analyses were performed to quantify human population kinetic variability in the human evaluation data set. The model identifies potential pharmacokinetic differences between rodents and humans, indicated by differences in model parameters between species. The PBPK model can be used to optimize the dosing regimen to improve oxime therapeutic efficacy in a human population.					
<b>15. SUBJECT TERMS</b> Oxime, PBPK model, Rat, Human, Pharmacokinetic, Organophosphate					
<b>16. SECURITY CLASSIFICATION OF:</b> U			<b>17. LIMITATION OF ABSTRACT</b> SAR	<b>18. NUMBER OF PAGES</b> 20	<b>19a. NAME OF RESPONSIBLE PERSON</b> Kyung O Yu
<b>a. REPORT</b> U	<b>b. ABSTRACT</b> U	<b>c. THIS PAGE</b> U			<b>19b. TELEPHONE NUMBER (Include area code)</b> 937-904-9504

Standard Form 298 (Rev. 8-98)  
Prescribed by ANSI-Std Z39-18

## A physiologically based pharmacokinetic model for the oxime TMB-4: simulation of rodent and human data

Teresa R. Sterner · Christopher D. Ruark ·  
Tammie R. Covington · Kyung O. Yu ·  
Jeffery M. Gearhart

Received: 6 June 2012 / Accepted: 21 November 2012 / Published online: 13 January 2013  
© Springer-Verlag Berlin Heidelberg (outside the USA) 2013

**Abstract** Multiple oximes have been synthesized and evaluated for use as countermeasures against chemical warfare nerve agents. The current U.S. military and civilian oxime countermeasure, 2-[(hydroxyimino)methyl]-1-methylpyridin-1-ium chloride (2-PAM), is under consideration for replacement with a more effective acetylcholinesterase reactivator, 1,1'-methylenebis[4-hydroxyiminomethyl]pyridinium dimethanesulfonate (MMB-4). Kinetic data in the scientific literature for MMB-4 are limited; therefore, a physiologically based pharmacokinetic (PBPK) model was developed for a structurally related oxime, 1,1'-trimethylenebis[4-hydroximinomethyl]pyridinium dibromide. Based on a previous model structure for the organophosphate diisopropylfluorophosphate, the model includes key sites of acetylcholinesterase inhibition (brain and diaphragm), as well as fat, kidney, liver, rapidly perfused tissues and slowly perfused tissues. All tissue compartments are diffusion limited. Model parameters were collected from the literature, predicted using quantitative structure–property relationships or, when necessary, fit to available pharmacokinetic data from the literature. The model was parameterized using rat plasma, tissue and urine time course data from intramuscular administration, as well as human blood and urine data from intravenous and intramuscular administration; sensitivity analyses were performed. The PBPK model successfully simulates rat and human data sets and has been evaluated by

predicting intravenous mouse and intramuscular human data not used in the development of the model. Monte Carlo analyses were performed to quantify human population kinetic variability in the human evaluation data set. The model identifies potential pharmacokinetic differences between rodents and humans, indicated by differences in model parameters between species. The PBPK model can be used to optimize the dosing regimen to improve oxime therapeutic efficacy in a human population.

**Keywords** Oxime · PBPK model · Rat · Human · Pharmacokinetic · Organophosphate

### Introduction

Traditional oximes are pyridinium mono- or bis-quaternary compounds characterized by their quaternary ammonium structures and low lipophilicity (negative log *P* values) (Voicu et al. 2010). Medically, oximes are administered to counteract organophosphate (OP) poisoning. OPs form serine-conjugated phosphonates or phosphorates with acetylcholinesterase (AChE). Oxime molecules bind to OP-AChE complexes and regenerate AChE activity through nucleophilic attack of the oximate on the phosphorus atom, leading to a pentacoordinate phosphoroxime-enzyme transition state. The unstable geometry of this complex liberates the enzyme from the phosphoroxime (Eyer 2003). The resulting reactivation of AChE enzymes restores cholinergic function disrupted by acetylcholine buildup in the post-synaptic clefts of neuromuscular junctions (Saxena et al. 2008).

While used in clinical practice as part of the treatment for OP pesticide exposure (Eddleston et al. 2008), effective oxime treatment is also a major concern for military

T. R. Sterner (✉) · C. D. Ruark · T. R. Covington ·  
J. M. Gearhart  
Henry M. Jackson Foundation for the Advancement  
of Military Medicine (HJF), 2729 R Street, Bldg 837,  
Wright-Patterson AFB, OH 45433-5707, USA  
e-mail: teri.sterner.ctr@wpafb.af.mil

K. O. Yu  
AFRL 711 HPW/RHDJ, Wright-Patterson AFB, OH, USA

members in the event of a chemical warfare nerve agent (CWNA) attack. 2-[(Hydroxyimino)methyl]-1-methylpyridin-1-ium chloride (2-PAM) has been fielded with U.S. troops since the 1970s (Saxena et al. 2008). The MARK I field kit, used by U.S. military and civilian agencies, is a double-barreled autoinjector containing a 2-mg atropine sulfate dose alongside a 600-mg dose of 2-PAM. Current military protocol is to use three MARK I kits as a loading dose in a severely affected victim, without exceeding 1,800 mg 2-PAM per hour. Also in the kit is a separate autoinjector containing 10 mg diazepam as an antidote for convulsions. Intramuscular autoinjectors allow for rapid self- or buddy-administration into a large muscle such as the thigh (Newmark 2009). Traditional oximes must be administered intravenously or intramuscularly because their oral uptake is poor, as indicated by the negative log P values. Oral bioavailability of several oximes, including 2-PAM, is only about 6 % of the intramuscular bioavailability (Voicu et al. 2010).

2-PAM is under consideration for replacement with a more effective AChE reactivator since the efficacy of 2-PAM is extremely limited against CWNAs such as soman (GD) and cyclosarin (GF) (Lundy et al. 2011; Saxena et al. 2008). A strong candidate for replacement is the symmetric bispyridinium oxime 1,1'-methylenebis{4-hydroxyimino-methyl}pyridinium dimethanesulfonate (methoxime or MMB-4) (Lundy et al. 2011). MMB-4 is effective against a broad range of OP CWNAs, including GD and GF, as well as other well-known agents such as tabun (GA), sarin (GB) and Russian VX (VR) (Koplovitz et al. 2007; Saxena et al. 2008). MMB-4 outperformed eight other oximes, including 2-PAM, in reactivating GB, GF, VX and VR-inhibited guinea pig AChE in blood, brain and three peripheral tissues (diaphragm, heart and skeletal muscle) (Shih et al. 2009). MMB-4, having a higher LD<sub>50</sub> in both rats and mice (Eyer and Worek 2007), is also less toxic than 2-PAM in these rodents. While MMB-4 is currently fielded in the Czech Republic, it has not been approved for use clinically in the United States (Lundy et al. 2011). For the U.S. military to deploy an antidote, it must undergo full approval by the U.S. Food and Drug Administration (FDA) (Newmark 2009).

Physiologically based pharmacokinetic models (PBPK) are uniquely suited for extrapolating kinetics between species, routes of administration and doses (Loizou et al. 2008), are essential for integrating in vitro animal data to optimize therapeutic dosing regimens in humans, and have even been used as a tool to facilitate FDA decisions (Zhao et al. 2011). Thus, in order to better understand potential species- and route-specific differences, a PBPK model for oximes was developed; however, development of a PBPK model requires pharmacokinetic data. Kinetic data for MMB-4 are limited at this time, but sufficient data are available for a closely related oxime, 1,1'-trimethylenebis{4-hydroxyiminomethyl}

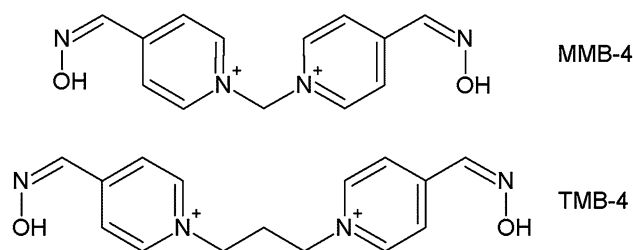


**Fig. 1** Chemical structures of MMB-4 and TMB-4

pyridinium dibromide (trimedoxime or TMB-4). TMB-4, while not as pharmacologically effective as MMB-4 against select agents (GB, GF, VX, VR) (Shih et al. 2009), is capable of activating OP-inhibited AChE and is actually more effective against GA in a human erythrocyte in vitro study (Kovarik et al. 2007). TMB-4 and MMB-4 are structurally similar (Fig. 1); therefore, in the absence of sufficient MMB-4 data, the oxime model was developed specifically for TMB-4 as a surrogate.

Developed herein is a PBPK model for TMB-4, using rat and human datasets from the literature. The model is evaluated against intravenous mouse and intramuscular human data not used in the original development of the model. Monte Carlo analyses are then utilized to quantify human population kinetic variability. Finally, sensitivity analyses are performed. This TMB-4 PBPK model can be expanded to include pharmacodynamics (PD), which would describe the interaction of OPs, AChE and oximes at the molecular level.

## Methods

MMB-4 and TMB-4 are water-soluble quaternary ammonium salts. TMB-4 is a kinetic surrogate for MMB-4 based not only on structure (Fig. 1), but also on predicted distribution parameters (Table 1). Log P, pKa and log D values predicted using ChemSketch (Advanced Chemistry Development, Inc., Toronto, Ontario, Canada) indicate high water solubility for both oximes. This property results in nearly identical predicted tissue/blood partition coefficients (PCs) for the two oximes (Table 1).

PCs are estimated using a modification of the quantitative structure–property relationship (QSPR) algorithm by Schmitt (2008) (Eq. 1):

$$K_{t,pl} = \frac{C_t}{C_{pl}} = \left(\frac{C_t}{C_u}\right) \left(\frac{C_u}{C_{pl}}\right) = \left(\frac{F_{int}C_{int} + F_{cell}C_{cell}}{C_u}\right) \left(\frac{C_u}{C_{pl}}\right) = \left(\frac{F_{int}}{f_u^{int}} + \frac{F_{cell}}{f_u^{cell}}\right) (f_u^{pl}) \quad (1)$$

where  $C_t$  is the chemical concentration in the tissue,  $C_{pl}$  is the chemical concentration in the plasma,  $C_u$  is the

**Table 1** Predicted distribution parameters for MMB-4 and TMB-4

Parameter	MMB-4		TMB-4	
Log P <sup>a</sup>	−1.87		−3.20	
pKa <sup>a</sup>	7.79		8.03	
Log D <sup>a,b</sup>	−1.22 to −1.13		−2.76 to −2.68	
Tissue/blood partition coefficients	Rat	Human	Rat	Human
Brain	0.91	0.92	0.91	0.92
Fat	0.27	0.24	0.21	0.19
Kidney	0.85	0.94	0.84	0.94
Liver	0.69	0.90	0.69	0.90
Muscle	0.89	0.94	0.89	0.94

<sup>a</sup> As predicted by ChemSketch

<sup>b</sup> Normal human blood pH is 7.32 to 7.43 (Wu 2006)

unbound chemical concentration,  $F_{int}$  is the fraction of tissue that is interstitium,  $C_{int}$  is the chemical concentration in the interstitium,  $F_{cell}$  is the fraction of tissue that is cellular,  $C_{cell}$  is the chemical concentration in the cellular space,  $f_u^{int}$  is the fraction of unbound chemical in the interstitium,  $f_u^{cell}$  is the fraction of unbound chemical in the cell and  $f_u^{pl}$  is the fraction of unbound chemical in the plasma.

The modification calculates the unbound chemical fraction,  $f_u$ , by accounting for the fraction of water in each respective tissue,  $F_w$ , based on the assumption that the unbound chemical is in the water fraction. Substituting into the Schmitt (2008) equation (Eq. 1) results in Eq. 2:

$$K_{t:pl} = \left( \frac{F_{int}C_{int} + F_{cell}C_{cell}}{C_u} \right) \left( \frac{C_u}{C_{pl}} \right) = \left( F_{int} \frac{F_w^{int}}{f_u^{int}} + F_{cell} \frac{F_w^{cell}}{f_u^{cell}} \right) \left( \frac{f_u^{pl}}{F_w^{pl}} \right) \quad (2)$$

where  $F_w^{int}$  is the fraction of water in the interstitium,  $F_w^{cell}$  is the fraction of water in the cellular space and  $F_w^{pl}$  is the fraction of water in the plasma. To convert  $K_{t:pl}$  to a steady state tissue/blood partition coefficient ( $K_{t:b}$ ), a red blood cell (RBC) compartment correction is made (Eq. 3):

$$K_{t:b} = \frac{K_{t:pl}}{(1 - F_{RBC}) + (K_{RBC:pl} \times F_{RBC})} \quad (3)$$

where  $F_{RBC}$  is the fraction of RBCs in blood, as determined from the hematocrit measurements, and  $K_{RBC:pl}$  is the steady state RBC/plasma partition coefficient.  $K_{RBC:pl}$  may be calculated using Eq. 2 where  $F_{int}$  is zero and  $F_{cell}$  is one.

#### PBPK model structure

PBPK models simulate the absorption, distribution, metabolism and excretion of chemicals. Groups of equations represent organs or grouped tissues that affect the

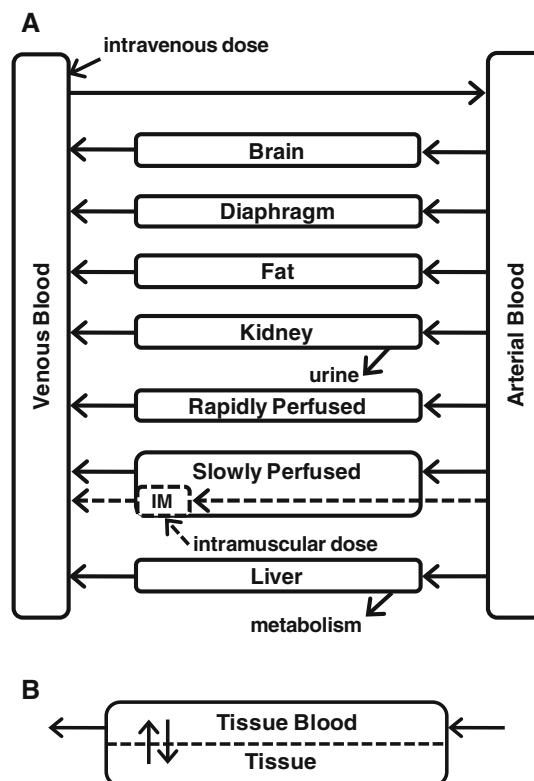


**Fig. 2** Schematic of the PBPK model structure for the oxime TMB-4. Tissue compartments depicted in Schematic a include diffusion limitation as illustrated by the generic tissue in Schematic b

pharmacokinetics of the chemical. The PBPK model presented here (Fig. 2) is based upon a previously published PBPK model for an OP, diisopropylfluorophosphate (DFP) (Gearhart et al. 1990, 1994). The model retains likeness to the DFP model in order to allow for future prediction of pharmacokinetic/pharmacodynamic interactions between OPs, oximes and AChE. The separate tissue compartments are described by a system of ordinary differential equations that are solved simultaneously using Gear's stiff algorithm implemented in acsIX (AEGIS Technologies, Huntsville, AL).

The TMB-4 model structure (Fig. 2) includes brain and diaphragm compartments, both of which are OP target tissues (Gearhart et al. 1990, 1994), and therefore, targets for oxime reactivation. The model also includes compartments for fat, kidney and liver, with the remaining organs lumped into rapidly and slowly perfused tissue compartments. Kidney and liver compartments represent not only locations for clearance of oximes, but are also tissues for which oxime time course data exist. Fat was kept separate from the slowly perfused tissues due to the extreme water solubility of oximes which would largely prevent their uptake into fat, but would not inhibit oximes from being taken up into more hydrophilic slowly perfused tissues such as muscle. Each compartment or tissue in the model (Fig. 2a) is coded with diffusion-limited distribution

(Fig. 2b) dependent not only on the tissue/blood PC, which regulates the concentration gradient–driven diffusion across the membranes, but also on the permeability area (PA) cross product for the tissue, which slows the penetration of molecules that do not readily diffuse.

The model uses Michaelis–Menten kinetics to describe both metabolism in the liver and excretion from the kidney. Minor amounts of TMB-4 metabolism have been shown by de Miranda et al. (1972) and Morgan et al. (1982). The model also incorporates saturable elimination kinetics as oximes are dependent on organic cation transporter (OCT) uptake in the proximal renal tubules to facilitate excretion (Shu 2011).

The model allows for TMB-4 dosing from intravenous and intramuscular routes. Intravenous injections are modeled as short infusions directly into the venous blood supply. The length of the injection is set to the study's actual infusion time, if reported, or fit to the data. A sub-compartment for intramuscular dosing (IM compartment) is separated from the slowly perfused tissue compartment as needed. The model simulates a concentrated amount of TMB-4 added quickly to a small portion of muscle. TMB-4 then diffuses into the venous blood directly, rather than coming to equilibrium in the entire slowly perfused compartment before diffusing into the blood. The length of the intramuscular injection is also set to study specifications, when published, or fit to the data. The volume of the IM compartment is calculated from the volume of the intramuscular injection in each study. This built-in flexibility allows the model to adapt to different dosing protocols. For intravenous dosing, the parameters for the IM compartment are set to zero, and the IM compartment is not separated from the slowly perfused tissue compartment.

TMB-4 is available in solid forms as the dibromide (Milic et al. 1996) and dichloride (Calesnick and Christensen 1967; Vojvodic 1970). Doses in the TMB-4 studies were reported as a dose of a specific salt or of the cation only. Therefore, all doses were converted to mg/kg body-weight (BW) of cation only, as needed, for use in the model. The oxime TMB-4 has a molecular weight of 286.33 g/mol without its anion. For simplicity, the model does not accommodate the different ionization states.

### Model parameterization

Physiological parameter values (Table 2) for each tissue were found in the published literature for each species (rat, mouse, human) whenever possible. Exceptions and calculated values are noted. When literature values were unavailable, parameters were fit using the model and the model parameterization data sets. All simulations use study-specific BW values. Allometric scaling (*i.e.*, volumes scaled by BW; flows and metabolic capacities scaled by

**Table 2** Physiological parameters used in the TMB-4 model

Parameter		Mouse	Rat	Human
Fraction hematocrit in blood	HEM	0.45 <sup>a</sup>	0.46 <sup>a</sup>	0.44 <sup>a</sup>
<i>Flow rates (L/h/kg<sup>0.75</sup>)</i>				
Cardiac output	QCC	16.22 <sup>b</sup>	14.09 <sup>b</sup>	12.89
Alveolar ventilation	QPC	29.091	19.856 <sup>b</sup>	12.396 <sup>b</sup>
<i>Blood flow rates (fraction of cardiac output)</i>				
Brain	QBrC	0.033	0.020	0.114
Diaphragm	QDC	0.006 <sup>c</sup>	0.006 <sup>c</sup>	0.006 <sup>d</sup>
Fat	QFC	0.070 <sup>e</sup>	0.070	0.052
Kidneys	QKC	0.091	0.141	0.175
Liver	QLC	0.161	0.183	0.227
Rapidly perfused*	QRC	0.59 <sup>f</sup>	0.47 <sup>f</sup>	0.66 <sup>f</sup>
Slowly perfused*	QSC	0.41 <sup>f</sup>	0.53 <sup>f</sup>	0.34 <sup>f</sup>
<i>Tissue volume (fraction of body weight)</i>				
Arterial blood	VAC	0.0122	0.0185	0.0308
Venous blood	VVC	0.0368	0.0555	0.0482
Brain	VBrC	0.017	0.006	0.020
Diaphragm	VDC	0.003 <sup>c</sup>	0.003 <sup>c</sup>	0.003 <sup>d</sup>
Fat	VFC	0.070	0.070	0.214
Kidneys	VKC	0.017	0.007	0.004
Liver	VLC	0.055	0.034	0.026
Rapidly perfused*	VRC	0.101 <sup>f</sup>	0.055 <sup>f</sup>	0.063 <sup>f</sup>
Slowly perfused*	VSC	0.793 <sup>f</sup>	0.821 <sup>f</sup>	0.844 <sup>f</sup>
<i>Tissue blood volume (fraction of tissue volume)</i>				
Brain	VBrBC	0.03	0.03	0.04
Diaphragm	VDBC	0.04 <sup>g</sup>	0.04 <sup>g</sup>	0.01 <sup>g</sup>
Fat	VFBC	0.015 <sup>h</sup>	0.015 <sup>h</sup>	0.020
Kidneys	VKBC	0.24	0.16	0.36
Liver	VLBC	0.31	0.21	0.11
Rapidly perfused	VRBC	0.208 <sup>i</sup>	0.208 <sup>i</sup>	0.170 <sup>i</sup>
Slowly perfused	VSBC	0.033 <sup>i</sup>	0.033 <sup>i</sup>	0.038 <sup>i</sup>
<i>IM compartment parameters</i>				
Blood flow rate (L/h/g)	QIMg	NA–iv only	0.012 <sup>j</sup>	0.045
Injection volume (mL)	VolIM	NA–iv only	0.25 <sup>k</sup>	2.00 <sup>l</sup>
Tissue blood volume (fraction)	VIMBC	NA–iv only	0.04 <sup>h</sup>	0.01 <sup>g</sup>

All values are from Brown et al. (1997) unless otherwise noted

<sup>a</sup> Davies and Morris (1993); <sup>b</sup> Arms and Travis (1988); <sup>c</sup> Gearhart et al. (1990); <sup>d</sup> Gearhart et al. (1994); <sup>e</sup> Rat value from Brown et al. (1997); <sup>f</sup> Sum of applicable tissue values published in Brown et al. (1997); <sup>g</sup> Muscle value from Brown et al. (1997); <sup>h</sup> Guinea pig value–Bosse and Wassermann (1970); <sup>i</sup> Average of applicable tissue values published in Brown et al. (1997); <sup>j</sup> Copp et al. (2010); <sup>k</sup> OCV (2011); <sup>l</sup> Vojvodic (1970)

\* Total flow or volume (*i.e.*, includes values for brain, fat, liver, etc.); the model subtracts the appropriate blood flows and tissue volumes from each lumped compartment following allometric scaling

BW to the three-quarters power) coded within the model was used to modify the inputs to accommodate interspecies extrapolation (Gearhart et al. 1990).

The IM compartment values in Table 2 are presented in different units due to the need to calculate the size and flow of the compartment based on the volume injected intramuscularly in each study. The blood flow to the rat IM compartment is set to a rate of 0.012 L/h/g tissue measured in the thigh muscle of control group Wistar rats (Copp et al. 2010). The fraction of cardiac output to the IM compartment is then calculated within the code based on the volume of the injection. The human muscle blood flow rate of 0.045 L/h/g muscle tissue is calculated from the fraction of cardiac output flow to muscle, the cardiac output flow rate and the fraction of BW that is muscle (Brown et al. 1997). The IM compartment volume is calculated in the code to be twice the volume of the injection; of this total volume, half is assumed to be muscle tissue and half is the injection solution. Although a more physiologically correct compartment would increase and decrease the volume with injection and subsequent absorption, this simplification helps capture the effect of the muscle fibers being swelled or separated to twice their normal size while retaining their original amount of blood flow.

Physicochemical parameters used in the model are summarized in Table 3. PCs for TMB-4 were initially set to QSPR estimates and were then refined as needed by fitting to the data. PCs were predicted for a variety of tissues for both rat and human (Table 2); rat PCs are also used for the mouse. Lumped compartment/blood PCs were calculated as averages of predicted values for rapidly (heart, lung) or slowly (muscle, skin, bone) perfused tissues. Diffusion limitation constants (permeability area cross products or PAs), metabolism and clearance parameters were fit to best describe the rat intramuscular data set (Garrigue et al. 1991).

#### Data used in model parameterization

Study data for parameterizing and evaluating the model are from the literature. A study was utilized if data were presented for blood or plasma time course from an intravenous or intramuscular dose of TMB-4 in any species. Only data where TMB-4 was administered alone were considered since it was assumed that co-administration with atropine would change the kinetics of the oxime due to its effects on the physiology of the animal (e.g., cardiac output).

Data from Garrigue et al. (1991) were selected to parameterize this PBPK model because the study measured time courses for plasma, urine and three tissues. In this study, male Wistar rats were administered a single intramuscular dose of <sup>14</sup>C-labeled TMB-4 equivalent to 21.5 mg/kg BW. Rats weighed 180 to 220 g; a midpoint of 200 g BW was utilized for model simulations. Animals

**Table 3** Physicochemical parameters used in the TMB-4 model

Parameter		Rat/ Mouse	Human
<i>Metabolism parameters</i>			
Maximum enzymatic metabolic rate constant (mg/h/kg <sup>0.75</sup> )	VMaxC	0.6 <sup>#</sup>	0.6*
Enzyme affinity constant (mg/L)	Km	0.1 <sup>#</sup>	0.1*
<i>Urinary excretion parameters</i>			
Maximum saturable excretion rate constant (mg/h/kg <sup>0.75</sup> )	VMaxUrC	80 <sup>#</sup>	480 <sup>#</sup>
Excretion affinity constant (mg/L)	KmUr	900 <sup>#</sup>	900*
<i>Dosing parameters</i>			
Length of intramuscular injection (hours)	TIM	0.025 <sup>#</sup>	0.0042 <sup>a</sup> 0.0083 <sup>b</sup>
Length of intravenous injection (hours)	TINF	0.01 <sup>c</sup>	0.0625 <sup>d</sup>
<i>Tissue/blood partition coefficients (unitless)<sup>e</sup></i>			
Brain	PBr	0.13 <sup>#</sup>	0.13*
Diaphragm	PD	0.89	0.94
Fat	PF	0.21	0.19
IM compartment	PIM	7.1 <sup>#</sup>	2.5 <sup>#</sup>
Kidney	PK	100 <sup>#</sup>	0.94
Liver	PL	12 <sup>#</sup>	0.90
Rapidly perfused	PR	0.73	0.97
Slowly perfused	PS	10 <sup>#</sup>	0.74
<i>Diffusion limitation coefficient constants (L/h/kg<sup>0.75</sup>)</i>			
Brain	PABrC	0.002 <sup>#</sup>	0.002*
Diaphragm	PADC	0.2 <sup>f</sup>	0.2*
Fat	PAFC	0.3 <sup>g</sup>	0.3*
IM compartment	PAIMC	12 <sup>#</sup>	12*
Kidney	PAKC	1.5 <sup>#</sup>	1.5*
Liver	PALC	0.2 <sup>#</sup>	0.2*
Rapidly perfused	PARC	1.5 <sup>h</sup>	1.5*
Slowly perfused	PASC	0.3 <sup>#</sup>	0.3*

<sup>a</sup> Fit for Vojvodic (1970); <sup>b</sup> Twice the value fit for Vojvodic (1970), corresponding to two injections in Calesnick and Christensen (1967);

<sup>c</sup> Fit for mouse simulation (Milic et al. 1996); <sup>d</sup> Calesnick and Christensen (1967) minimum study value; <sup>e</sup> PC values predicted unless otherwise noted; <sup>f</sup> Set to liver fit value; <sup>g</sup> Set to slowly perfused tissue fit value; <sup>h</sup> Set to kidney fit value

# Fit value; \* Value from rat model

were euthanized at set time points and plasma, urine, liver, kidney and brain samples were taken.

Milic et al. (1996) administered an intravenous dose of 16.03 mg TMB-4/kg BW to male albino mice and recorded the plasma time course. The mice weighed 24–30 g; a midpoint value of 27 g was used for model simulations. This study allows a limited evaluation of the rodent parameterization of the model in which all model inputs were the same as for the rat with the exception of physiological parameters. The study also allows for verification that the model code can simulate intravenous dosing.

Following the rodent evaluation, the model was parameterized with two available human data sets. Intravenous data from Calesnick and Christensen (1967) were useful in fitting the IM compartment PC and saturable urinary clearance parameters for humans. In this study, a volunteer was administered 24.05 mg TMB-4/kg BW intravenously. The number of subjects was not explicitly stated, so a single volunteer is assumed per time point, as standard deviations are not provided in the study. Male and female volunteers ranged in age from 23 to 64 years old with body weights ranging from 39.5 to 86.2 kg; a mid-point value of 62.85 kg was used for model simulations. The reported duration of intravenous infusion (TInf) ranged from 0.0625 to 0.25 h. Whole-blood time course samples at various times over an 8-h period and a 24-h cumulative urine specimen were collected.

A second study was available for use in human parameterization. In the Vojvodic (1970) study, male volunteers with a mean body weight of 81.89 kg were dosed intramuscularly with 200 mg of TMB-4 (approximately 2.45 mg TMB-4/kg BW) in 2 mL of saline. Whole-blood time course and cumulative urine amounts over 4 h were recorded. This study is useful in setting the IM compartment/blood PC for humans and fitting early time points for urinary excretion.

For limited evaluation of the human parameters, an intramuscular data set from the Calesnick and Christensen (1967) study was utilized. A volunteer was injected intramuscularly with 12.02 or 24.05 mg TMB-4/kg BW in 15 mL of sterile water. Half of the total volume of the injection (7.5 mL) was given in each buttock. The length of the injections (TIM) was set to twice the value fit for the Vojvodic (1970) study, as it was assumed the injections were administered one after the other.

#### Monte Carlo analyses

Monte Carlo (MC) analyses are used to evaluate variability in model predictions and were conducted utilizing the Calesnick and Christensen (1967) human intramuscular study parameters. Physiological parameters are described with a normal distribution while physicochemical parameters (PC, PA, VMaxC and Km values) are described with a lognormal distribution (Covington et al. 2007). Coefficients of variation were set using published values, except as noted in Table 4. Bounds were defined as  $\pm$  two standard deviations (SD), except in specific cases. The BW bounds were set to the published range for the Calesnick and Christensen (1967) study (39.5–86.2 kg) with the analysis mean being equal to the midpoint value of the data range (62.85 kg). Blood flow rates and tissue volumes for the slowly and rapidly perfused tissues, as shown in Table 4, are not the same as those listed in Table 1; the mean for each of these

values represents the value calculated by the model after subtracting the appropriate blood flows and tissue volumes from each lumped compartment. The bounds were then set using the post-calculation number to keep an MC analysis from choosing a lumped value that is smaller than one of the component tissues. The metabolic enzyme and urinary excretion affinity constant bounds (Km and KmUr, respectively) were also set to avoid zero values, which would cause the Michaelis–Menten equation to divide by zero, the saturable pathways to turn off, and metabolism and excretion to no longer be concentration dependent. The model was run for 1,000 iterations with all physiological and physicochemical parameters varied randomly within the defined distributions.

An MC analysis may select fractional values such that they no longer sum in a physiological manner (e.g., fractional blood flows summing to more than 1). Since mass balance must be maintained, the randomly selected fractional blood flows and tissue volumes are “rebalanced” by adjusting each parameter in a fractional manner such that they sum to the correct total.

#### Sensitivity analysis

Sensitivity analyses determine to which parameters the model is most responsive. They also help identify inconsistencies within the model and determine which critical parameters may require further research (Kohn 2002; Loizou et al. 2008). Sensitivity analyses were conducted in order to determine the impact on selected endpoints of varying input parameters by 1 %. These analyses were conducted by increasing each parameter sequentially by 1 % and calculating the resulting sensitivity coefficient (SC) for each time point as the increase in the endpoint over the baseline endpoint value (*i.e.*, with none of the input parameters varied) divided by the increase in parameter value over baseline parameter value. Parameters were varied one at a time and were returned to their original values before the next parameter was varied. Differences for SCs were calculated using the central difference method and were normalized to both the response variable as well as the parameter being varied.

Sensitivity analyses were run to simulate kinetics for 3 h post-dosing due to the relatively short therapeutic window for oximes. Venous blood and brain concentration were selected as the response variables as sufficient oxime concentrations in the blood and target tissues are of foremost concern for achieving effective AChE reactivation. Human study parameters from Calesnick and Christensen (1967) and Vojvodic (1970) were used to evaluate intravenous and intramuscular routes, respectively. Parameters were considered to be sensitive if the SC exceeded 0.5, in absolute value, meaning that the output parameter changed

**Table 4** Distribution definitions for human Monte Carlo analysis of Calesnick and Christensen (1967) intramuscular data

Parameter		Distribution				
		Shape	Mean	CV <sup>a</sup> (%)	Bounds	
					Lower	Upper
Body weight (kg)	BW	Normal	62.85 <sup>b</sup>	30	39.5 <sup>c</sup>	86.2 <sup>c</sup>
<i>Flow rates (L/h/kg<sup>0.75</sup>)</i>						
Cardiac output	QCC	Normal	12.89	9 <sup>d</sup>	10.57	15.21
Ventilation perfusion ratio (QCC/QPC)	VPR	Lognormal	0.962	15	0.673	1.251
<i>Blood flow rates (fraction of cardiac output)</i>						
Brain	QBrC	Normal	0.114	20 <sup>e</sup>	0.068	0.160
Diaphragm	QDC	Normal	0.006	15 <sup>f</sup>	0.004	0.008
Fat	QFC	Normal	0.052	30	0.021	0.083
Kidneys	QKC	Normal	0.175	35	0.053	0.298
Liver	QLC	Normal	0.227	35	0.068	0.386
Rapidly perfused	QRC	Normal	0.144	20	0.086	0.202
Slowly perfused	QSC	Normal	0.282	15	0.197	0.367
<i>Tissue volume (fraction of body weight)</i>						
Arterial blood	VAC	Normal	0.0308	10 <sup>e</sup>	0.0246	0.0370
Venous blood	VVC	Normal	0.0482	10 <sup>e</sup>	0.0386	0.0578
Brain	VBrC	Normal	0.020	10 <sup>e</sup>	0.016	0.024
Diaphragm	VDC	Normal	0.003	30 <sup>f</sup>	0.001	0.005
Fat	VFC	Normal	0.214	30	0.086	0.342
Kidneys	VKC	Normal	0.004	5	0.0036	0.0044
Liver	VLC	Normal	0.026	5	0.023	0.029
Rapidly perfused	VRC	Normal	0.013 <sup>g</sup>	10	0.010	0.016
Slowly perfused	VSC	Normal	0.627 <sup>g</sup>	30	0.251	0.9 <sup>c</sup>
<i>Tissue blood volume (fraction of tissue volume)</i>						
Brain	VBrBC	Normal	0.04	10 <sup>h</sup>	0.032	0.048
Diaphragm	VDBC	Normal	0.01	30 <sup>h</sup>	0.004	0.016
Fat	VFBC	Normal	0.020	30 <sup>h</sup>	0.008	0.032
Kidneys	VKBC	Normal	0.36	5 <sup>h</sup>	0.32	0.40
Liver	VLBC	Normal	0.11	5 <sup>h</sup>	0.10	0.12
Rapidly perfused	VRBC	Normal	0.170	10 <sup>h</sup>	0.136	0.204
Slowly perfused	VSBC	Normal	0.038	30 <sup>h</sup>	0.015	0.060
<i>IM compartment parameters</i>						
Blood flow rate (L/h/g)	QIMg	Normal	0.0045	15 <sup>f</sup>	0.0032	0.0059
Tissue blood volume (fraction)	VIMBC	Normal	0.01	30 <sup>f,h</sup>	0.004	0.016
<i>Metabolism parameters</i>						
Maximum enzymatic metabolic rate constant (mg/h/kg <sup>0.75</sup> )	VMaxC	Lognormal	0.6	30 <sup>d</sup>	0.2	1.0
Enzyme affinity constant (mg/L)	Km	Lognormal	0.1	50 <sup>d</sup>	0.001 <sup>c</sup>	0.2
<i>Urinary excretion parameters</i>						
Maximum saturable excretion rate constant (mg/h/kg <sup>0.75</sup> )	VMaxUrC	Lognormal	480.0	30 <sup>i</sup>	192.0	768.0
Excretion affinity constant (mg/L)	KmUr	Lognormal	900.0	50 <sup>i</sup>	1.0 <sup>c</sup>	1800.0
<i>Tissue/blood partition coefficients (unitless)</i>						
Brain	PBr	Lognormal	0.13	20	0.08	0.18
Diaphragm	PD	Lognormal	0.94	20	0.56	1.32
Fat	PF	Lognormal	0.19	30	0.08	0.30
IM compartment	PIM	Lognormal	2.5	20	1.5	3.5
Kidney	PK	Lognormal	0.94	20	0.56	1.32
Liver	PL	Lognormal	0.90	20	0.5	1.3

**Table 4** continued

Parameter		Distribution				
		Shape	Mean	CV <sup>a</sup> (%)	Bounds	
					Lower	Upper
Rapidly perfused	PR	Lognormal	0.97	20	0.58	1.36
Slowly perfused	PS	Lognormal	0.74	20	0.44	1.04
<i>Diffusion limitation coefficient constants (L/h/kg<sup>0.75</sup>)</i>						
Brain	PABrC	Lognormal	0.002	20 <sup>j</sup>	0.001	0.003
Diaphragm	PADC	Lognormal	0.2	20 <sup>j</sup>	0.1	0.3
Fat	PAFC	Lognormal	0.3	30 <sup>j</sup>	0.1	0.5
IM compartment	PAIMC	Lognormal	12.0	20 <sup>j</sup>	7.0	17.0
Kidney	PAKC	Lognormal	1.5	20 <sup>j</sup>	0.9	2.1
Liver	PALC	Lognormal	0.2	20 <sup>j</sup>	0.1	0.3
Rapidly perfused	PARC	Lognormal	1.5	20 <sup>j</sup>	0.9	2.1
Slowly perfused	PASC	Lognormal	0.3	20 <sup>j</sup>	0.2	0.4

<sup>a</sup> Coefficient of variation (CV) values from Covington et al. (2007) unless otherwise specified; <sup>b</sup> Calesnick and Christensen (1967) mid-range BW value; <sup>c</sup> Altered bounds (see text); <sup>d</sup> Clewell et al. (2001); <sup>e</sup> Rapidly perfused tissue CV; <sup>f</sup> Slowly perfused tissue CV; <sup>g</sup> Does not represent total flow or volume as in Table 1 (see text); <sup>h</sup> Same CV as for tissue volume compartment; <sup>i</sup> Same CV as for saturable metabolism parameter; <sup>j</sup> Same CV as for corresponding partition coefficient

half as much as the input parameter was varied. A parameter was considered very sensitive if the SC in absolute value exceeded 1.0.

## Results

### Rat model simulations

The TMB-4 PBPK model was developed using data from Garrigue et al. (1991) which were collected from Wistar rats dosed intramuscularly with 21.5 mg radiolabeled TMB-4/kg BW. Model simulations of plasma, tissue and cumulative urine time course data are shown in Fig. 3; overall, these simulations fit the available data well with minor exceptions. The model predicts a slightly earlier peak in the plasma concentration and somewhat over-predicts the tail of the plasma time course (Fig. 3a). Simulated brain and liver concentrations closely match the available data (Fig. 3b, c) while kidney concentration is over-predicted at the early (10 min) time point (Fig. 3b). Standard deviations were not available for plasma or tissue data to determine whether the model predictions lie within the data variability. Predicted urinary elimination falls within one standard deviation of the mean at every time point, indicating reasonable estimation of urinary excretion of TMB-4 in rats (Fig. 3d).

In order to obtain these predictions, the model required larger values for kidney/blood, liver/blood and slowly perfused tissue compartment/blood PCs (100.0, 12.0 and 10.0, respectively) versus the smaller predicted values (0.84, 0.69 and 0.71, respectively). Conversely,

the model required a smaller brain/blood PC (0.13) compared to the predicted value (0.91). The length of the injection (TIM), the PA values and the tissue/blood PC for the IM compartment were also fit for the Garrigue et al. (1991) data.

### Evaluation of model and rodent parameters

Since only two sets of rodent time course kinetic data for TMB-4 were found in the literature, the remaining data set (Milic et al. 1996) was used for limited evaluation of the model. Milic et al. (1996) published plasma time course concentrations for mice dosed intravenously with 16.03 mg TMB-4/kg BW. The model is able to predict these plasma time course data (Fig. 4) utilizing mouse physiological parameters (Table 2) and rat physicochemical parameters (Table 3). It was necessary to fit the length of intravenous infusion (TInf), as this is not stated within Milic et al. (1996). The injection duration was set to 0.01 h. Over-prediction of the first time points occurs because the model assumes instant mixing of venous blood. The model under-predicts mouse plasma TMB-4 levels in the tail of the time course. Overall, the evaluation of the model indicates a successful prediction utilizing the rat parameters for a similar species (mouse).

### Human model simulations

The model demonstrates its ability to be used for interspecies extrapolation by predicting whole-blood concentrations and cumulative urinary elimination data for humans with

**Fig. 3** Model simulations (lines) for **a** plasma, **b** kidney (dashed line and open triangles), liver (solid line and closed triangle) and **c** brain concentrations, and **d** cumulative urinary excretion compared with measured rat data (symbols, mean  $\pm$  1 SD) from Garrigue et al. (1991). Rats were administered a single intramuscular dose of  $^{14}\text{C}$ -labeled TMB-4 equivalent to 21.5 mg/kg BW

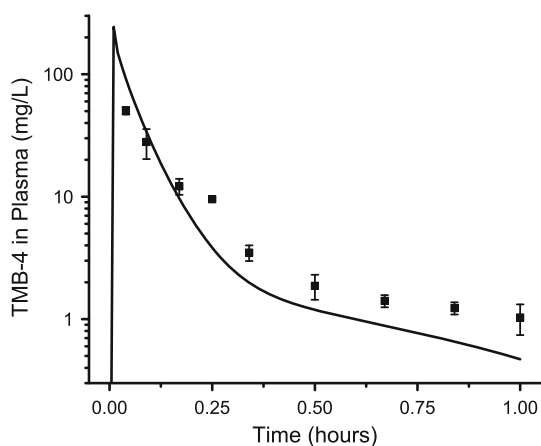
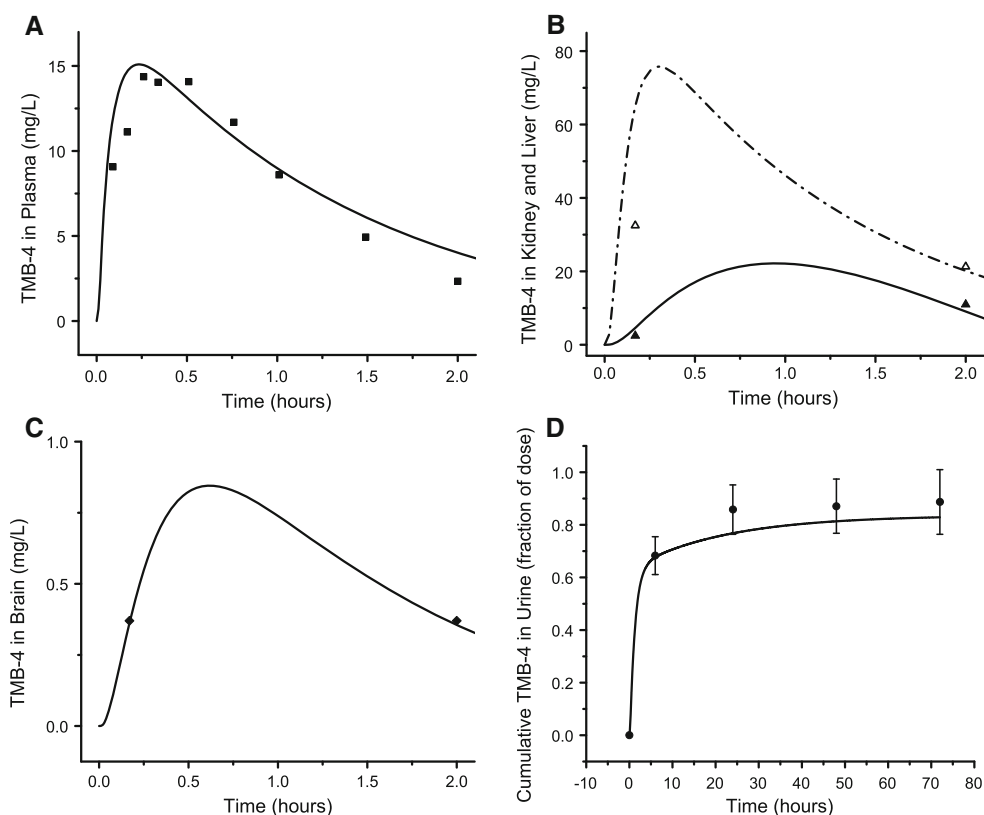


**Fig. 4** Model simulation (line) of plasma concentration compared with measured mouse data (symbols, mean  $\pm$  1 SD) from Milic et al. (1996). Mice received an intravenous dose of 16.03 mg TMB-4/kg BW

relatively few parameter adjustments. Intravenous data from Calesnick and Christensen (1967) and intramuscular data from Vojvodic (1970) were used to parameterize the model for human kinetics. The change in species necessitated alterations to the maximum rate constants for metabolism and excretion ( $V_{\text{MaxC}}$ ,  $V_{\text{MaxUrC}}$ ). In addition, dose route parameters, including the IM compartment/blood PC (PIM) and the lengths of intramuscular and intravenous

infusions (TIM, TInf), are altered to fit not only the changed physiology, but also study protocol differences.

Predicted PC values were largely utilized for the human parameterization of the TMB-4 model. Tissue/blood PC values for the liver, kidney and slowly perfused tissues, previously fit to the rat data, were returned to QSPR-predicted levels for the human data sets. The brain/blood PC remained the same as the fit value (0.13) from the Garrigue et al. (1991) rat data due to the lack of human brain data. The IM compartment/blood PC was fit using the Vojvodic (1970) data; visual fitting to these intramuscular data results in a tissue/blood PC of 2.5 for the IM compartment. The human parameterization used rat PA values.

The model is able to simulate the Calesnick and Christensen (1967) intravenous whole-blood data well (Fig. 5a). The volunteer was administered 24.05 mg TMB-4/kg BW intravenously. The length of injection (TInf) is set to the minimum study value (0.0625 h) as it best simulated the data curve. The model under-predicts the mean 24-h urinary output by 12 % (Fig. 5b). Rather than fitting excretion parameters to this single data point, the data from Vojvodic (1970) were utilized to set the parameters for this endpoint.

The Vojvodic (1970) data set was utilized for fitting human excretion rates and intramuscular administration parameter values. The model fits the whole-blood time course and the cumulative urinary elimination data well (Fig. 6). Standard deviation values were only available for

the blood time course and illustrate the variability of TMB-4 blood concentrations between individuals. The model is capable of simulating the urinary excretion curve at early time points which cannot be determined for rats due to the lack of early data.

#### Evaluation of human parameters and Monte Carlo analyses

To evaluate the human TMB-4 model parameterization, an intramuscular data set of TMB-4 blood levels from the Calesnick and Christensen (1967) study was reserved. In the intramuscular portion of this study, a volunteer was administered 12.02 or 24.05 mg TMB-4/kg BW. The model reasonably predicts the low dose whole-blood data (Fig. 7a) with the exception of the curious flatness of the data at early time points not seen previously in the rat (Fig. 3) or the human (Fig. 6) intramuscular data of Vojvodic (1970). The model uniformly under-predicts the higher intramuscular dose by approximately 20 % (Fig. 7b).

To evaluate the effect of normal human variability on model predictions, Monte Carlo analyses were performed. Calesnick and Christensen (1967) accepted 11 male and 29 female volunteers ranging greatly in age (23–64 years) and body weight (39.5–86.2 kg). Figure 7 shows the results of the MC analyses of the Calesnick and Christensen (1967) human intramuscular study using the study BW range (39.5–86.2 kg) as bounds for that parameter distribution and the midpoint of that range (62.85 kg) as the mean for the distribution. The MC estimates show that the observed data from one or more volunteers per dose fell within 2 SD of model predicted values, reflecting a fit within 95 % of normal human population variability given the body weight range specified.

Calesnick and Christensen (1967) report a 24-h elimination of just 34 % for both the high and low doses. This low level of elimination is not seen in the rat data above, nor in the human intravenous and other human

intramuscular data sets previously presented; therefore, predictions of these apparently anomalous data are not attempted.

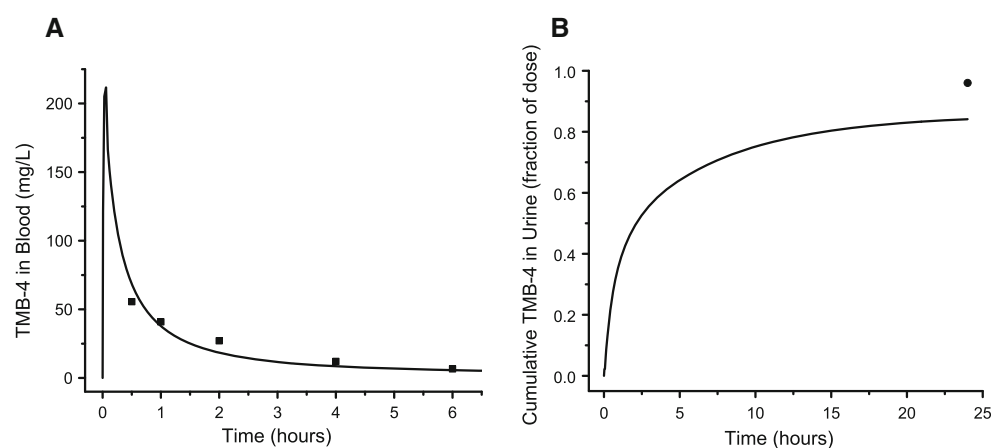
#### Sensitivity analysis

The model is sensitive to several parameters over a 3-h simulation. The endpoints of concern for the sensitivity analysis are TMB-4 blood and brain concentrations. Both intravenous and intramuscular dosing routes were analyzed; all physiological and physicochemical inputs into the model were varied. SC ranges are listed for each sensitive and very sensitive parameter by route and endpoint in Table 5.

The blood concentration of TMB-4 administered by the intravenous route is sensitive to six parameters. Figure 8a shows two of the physiological parameters to which the blood concentration is sensitive: the volume of the slowly perfused tissue compartment (VSC) and the volume of venous blood (VVC). The model is sensitive to VVC only during the initial distribution phase; the model is sensitive to VSC initially and again during the end of the critical 3-h time period. Figure 8b shows the SC time courses of an administration parameter, length of intravenous injection (TInf), to which the model is sensitive only during the administration of TMB-4. Three physicochemical parameter SC time courses (the kidney/blood PC (PK), the maximum saturable excretion rate constant (VMaxUrC) and the excretion affinity constant (KmUr)) are also shown in Fig. 8b. These parameters affect kidney uptake and excretion, and their variance results in model sensitivity in the latter half of the 3-h time course.

The brain concentration of TMB-4 by the intravenous route is sensitive to the same physiological and administration parameters as the blood concentration. Again, this endpoint is sensitive to VVC (Fig. 9a) and TInf (Fig. 9b) during the initial distribution of TMB-4; however, brain concentration is sensitive to VSC for almost the entire 3-h

**Fig. 5** Model simulations (lines) compared with measured human intravenous data (symbols) for **a** whole-blood time course and **b** cumulative urinary excretion from Calesnick and Christensen (1967). Volunteers were administered 24.05 mg TMB-4/kg BW



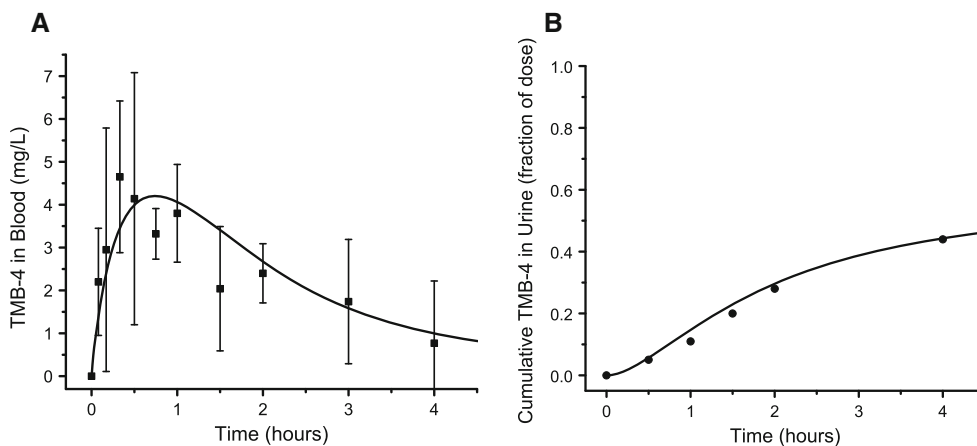


**Fig. 6** Model simulations (*lines*) compared with measured human intramuscular data (*symbols*, mean  $\pm$  1 SD, when available) for **a** whole-blood time course and **b** cumulative urinary excretion from

Vojvodic (1970). Male volunteers were dosed intramuscularly with 2.45 mg TMB-4/kg BW

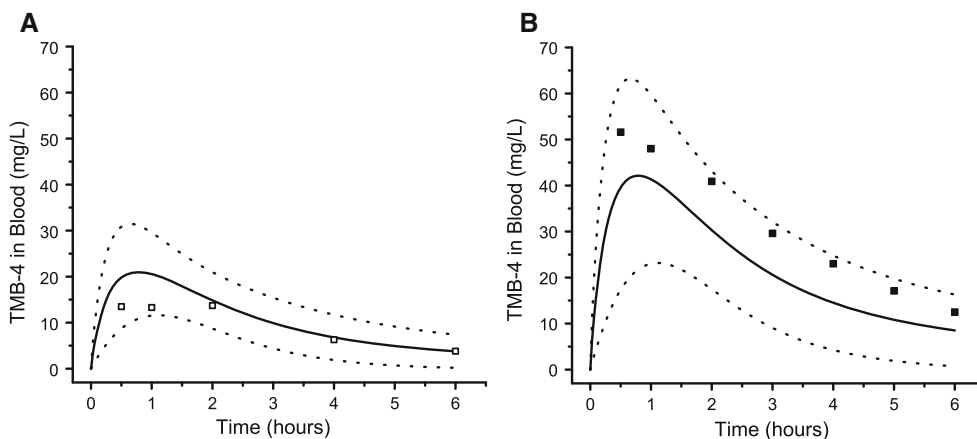


**Fig. 7** Monte Carlo estimates of variability of blood concentration (*lines*) compared with measured human intramuscular data (*symbols*) from Calesnick and Christensen (1967). Average predictions from 1000 simulations (*solid line*) are shown as well as  $\pm$  two SD

predictions (*dotted line*) which encompass 95 % of human variability. Volunteers were administered intramuscular doses of **a** 12.02 or **b** 24.05 mg TMB-4/kg BW

time period (Fig. 9a). Brain concentration was also sensitive to five additional parameters. Sensitivity is shown to three more physiological parameters (cardiac output (QCC), volume of arterial blood (VAC) and volume of the brain (VBrC)) (Fig. 9a). Sensitivity to QCC and VAC occur only initially, while brain concentration is sensitive to VBrC throughout most of the 3 h. Variance of two physicochemical parameters (the brain/blood PC (PBr) and brain diffusion limitation coefficient constant (PABrC)) result in sensitivity of this endpoint as well (Fig. 9b). The model is sensitive to PABrC throughout most of the 3 hours, while it is sensitive to PBr only at the very end of the evaluated time period. Brain concentration output was found to be very sensitive to only two of these eight parameters, VSC and VBrC, by the criteria of SC values greater in absolute value than 1.0.

The blood concentration endpoint for the intramuscular route was found to be sensitive to only four parameters. Again, VVC and VSC were two of the physiological parameters; this endpoint was sensitive to VVC at the very beginning of distribution of the drug and was sensitive to VSC during the first and last portions of the time course (Fig. 10). Blood concentration was sensitive to another physiological parameter (blood flow to the IM compartment (QIMg)) and a physicochemical parameter (the IM compartment/blood PC); variance of these two route-specific parameters resulted in sensitivity only during the first hour of the time course. The model was very sensitive to variance of only one parameter, VSC.

Finally, the brain concentration of TMB-4 following intramuscular administration was sensitive to 12 parameters. As with all of the other analyses, brain concentration

**Table 5** Minimum and maximum sensitivity coefficient (SC) values for human intravenous and intramuscular sensitivity analyses

Parameter		Endpoint			
		Intravenous concentration		Intramuscular concentration	
		Blood	Brain	Blood	Brain
Body weight	BW	NS	NS	NS	<b>-0.624</b> , 0.060
<i>Flow rates</i>					
Cardiac output	QCC	NS	-0.085, <b>0.889</b>	NS	-0.082, <b>1.52</b>
<i>Blood flow rates</i>					
Blood flow to brain	QBrC	NS	NS	NS	0, <b>0.671</b>
Blood flow to IM compartment	QIMg	NA	NA	-0.413, <b>0.999</b>	0.255, <b>0.999</b>
Blood flow to rapidly perfused tissues	QRC	NS	NS	NS	-0.044, <b>0.554</b>
<i>Tissue volume</i>					
Volume of arterial blood	VAC	NS	<b>-0.633</b> , 0.008	NS	<b>-0.756</b> , 0.009
Volume of brain	VBrC	NS	<b>-1.32</b> , -0.435	NS	<b>-1.65</b> , <b>-0.585</b>
Volume of slowly perfused tissues	VSC	<b>-0.579</b> , <b>0.620</b>	0.411, <b>2.49</b>	<b>-0.590</b> , <b>1.62</b>	<b>0.821</b> , <b>3.92</b>
<i>Tissue blood volume</i>					
Volume of venous blood	VVC	<b>-0.620</b> , 0.122	<b>-0.668</b> , 0.012	<b>-0.786</b> , 0.063	<b>-0.710</b> , 0.013
Volume of brain blood	VBrBC	NS	NS	NS	<b>-0.625</b> , 0.032
<i>Urinary excretion parameters</i>					
Maximum saturable excretion rate constant	VMaxUrC	<b>-0.771</b> , 0	NS	NS	NS
Excretion affinity constant	KmUr	0, <b>0.752</b>	NS	NS	NS
<i>Tissue/blood partition coefficients</i>					
Brain/blood PC	PBr	NS	0, <b>0.551</b>	NS	NS
IM compartment/blood PC	PIM	NA	NA	<b>-0.987</b> , 0.414	<b>-0.987</b> , -0.254
Kidney/blood PC	PK	<b>-0.744</b> , -0.001	NS	NS	NS
<i>Diffusion limitation coefficient constants</i>					
Brain diffusion limitation					
Coefficient constant	PABrC	NS	0.444, <b>0.998</b>	NS	<b>0.604</b> , <b>0.999</b>
<i>Administration route parameter</i>					
Duration of injection (intravenous or intramuscular)	TInf or TIM	<b>-0.991</b> , <b>0.505</b>	<b>-0.990</b> , <b>0.983</b>	NS	NS

Bold SC values are > |0.5|; Underlined SC values are > |1.0|

NA not applicable to the route, NS not sensitive

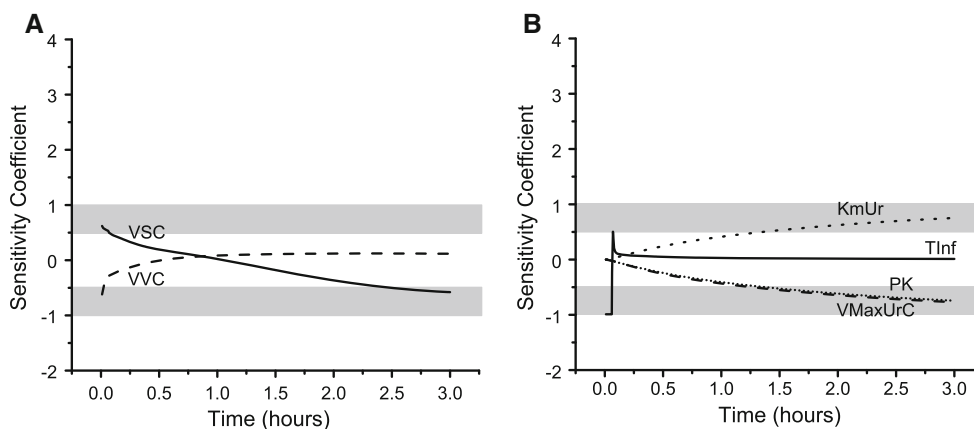


**Fig. 8** Time courses of sensitivity coefficients for six model parameters to which model predictions of TMB-4 blood concentration are sensitive following intravenous administration

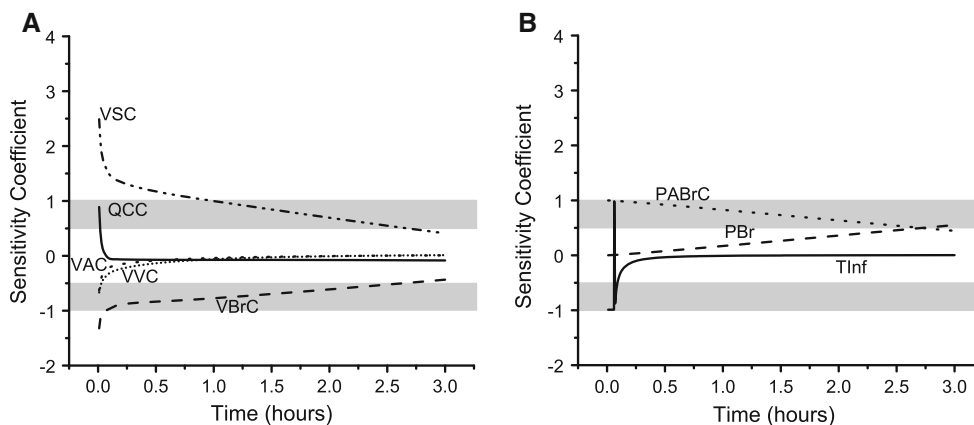


**Fig. 9** Time courses of sensitivity coefficients for eight model parameters to which model predictions of TMB-4 brain concentration are sensitive following intravenous administration

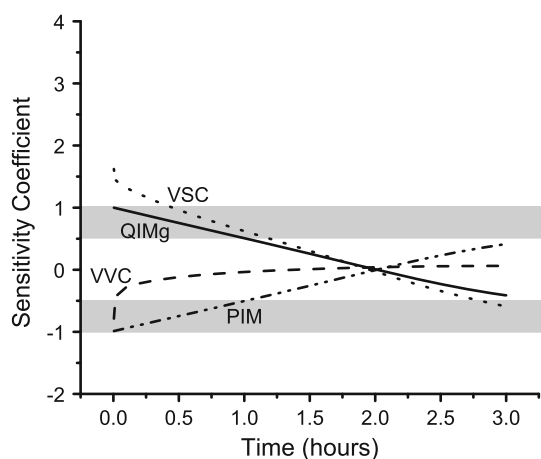


**Fig. 10** Time courses of sensitivity coefficients for four model parameters to which model predictions of TMB-4 blood concentration are sensitive following intramuscular administration

was sensitive to changes in VVC and VSC (Fig. 11a). This endpoint was sensitive to VVC early in the time course and was sensitive to VSC throughout the 3-h period. The endpoint was sensitive to QCC and VAC (Fig. 11a) in the manner previously seen in Fig. 9a for the intravenous analysis. Sensitivity was also shown to QIMg and PIM, in an equal and opposite manner (Fig. 11b), as shown for the blood endpoint in Fig. 10. The intramuscular endpoint analysis revealed sensitivity to two additional physiological parameters: the blood flow to the rapidly perfused tissue compartment (QRC) and BW (Fig. 11b). Both were only significant in the early distribution stage of the 3-h analysis. Finally, the brain concentration of TMB-4 was sensitive to four brain parameters (Fig. 11c), of which only PABrC was seen in the intravenous analysis (Fig. 9b). The intramuscular analysis showed sensitivity to blood flow to the brain (QBrC) and volume of blood in brain tissue (VBrBC), both early in the time course (Fig. 11c). The

volume of the brain itself (VBrC) was a sensitive parameter throughout the time course in this analysis. Variance of three parameters, QCC, VBrC and VSC, resulted in very sensitive SC values by the chosen criterion.

## Discussion

The model presented here is the first published PBPK model of an oxime. Previous kinetic models of oximes utilized one- and two-compartment models to simulate blood concentrations for individual studies (Stemler et al. 1991; Worek et al. 2005). A PBPK model has the advantage of interspecies and cross-route extrapolation. This PBPK model was initially developed to predict plasma and tissue time course and urinary elimination data following intramuscular administration of the oxime TMB-4 in rats. The model was then evaluated with mouse intravenous data. Following initial development, the model was parameterized for humans utilizing intravenous and intramuscular data and evaluated using additional human intramuscular data. The PBPK model structure incorporates multiple tissues important to the administration, distribution, metabolism and elimination of oximes. The structure also includes target tissues for OP action and oxime reactivation of AChE activity (brain, diaphragm), which will be useful in tying the TMB-4 model to an OP model for future PBPK and pharmacodynamic model development.

Also incorporated in the model structure is an intramuscular dosing compartment. The IM compartment is different from the other model compartments in two ways: (1) it is created within the model code only with an intramuscular dose and (2) the model calculates the size of the compartment based on the volume of the dose. The design of this compartment allows the model to more correctly simulate different dose volumes, which ranged in humans

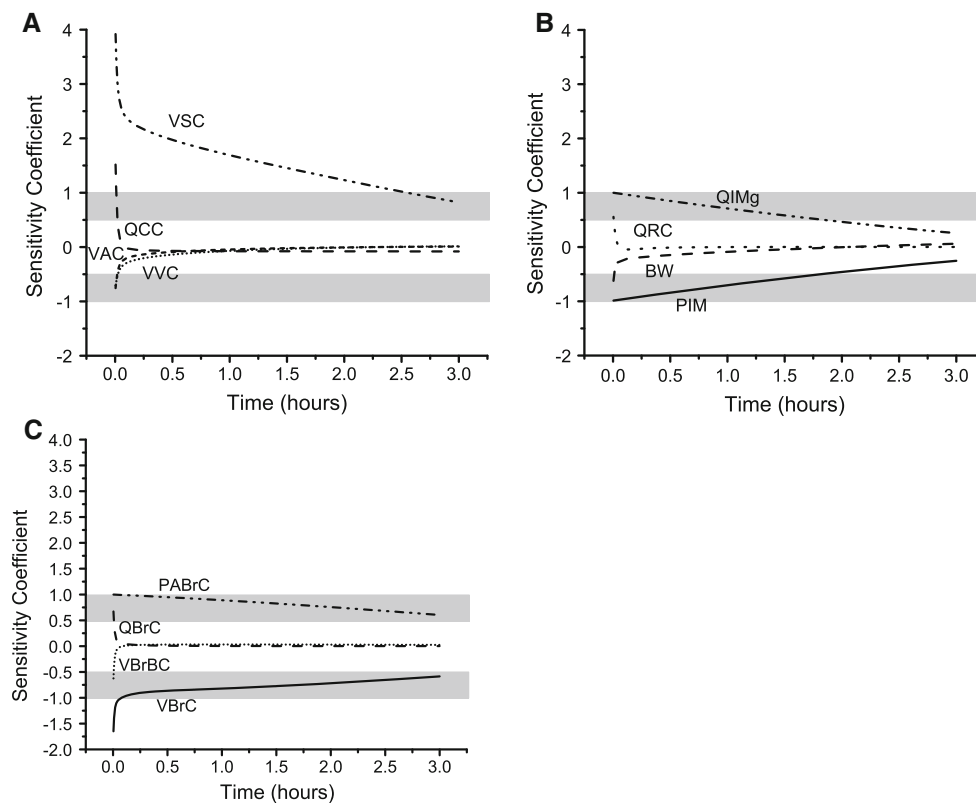


**Fig. 11** Time courses of sensitivity coefficients for 12 model parameters to which model predictions of TMB-4 brain concentration are sensitive following intramuscular administration

from 2 mL (Vojvodic 1970) to 15 mL (Calesnick and Christensen 1967). Dosing and absorption via the IM compartment are dependent upon the length of time for the injection (TIM), the volume of the injection (VolIM), the blood flow to the injection site (QIMg) and the partition coefficient of the IM compartment (PIM). Separate values for PIM were fit for rodents and humans. A single human value was used to simulate the model development data (Vojvodic 1970) and predict the limited evaluation data (Calesnick and Christensen 1967 data) with reasonable results.

The IM compartment designed for this model is unlike those in previously published models. The DFP model on which this project was based (Gearhart et al. 1994) added the dose directly into the slowly perfused tissue compartment, using an artificially slow injection rate to regulate the speed of chemical absorption. Another model utilized a sub-compartment of the slowly perfused tissues for the purpose of intramuscular dosing (Chen and Seng 2012); however, it modeled absorption from this sub-compartment as going to the larger slowly perfused tissues compartment rather than directly into the blood, which would still require the drug concentration to come to equilibrium with the entire slowly perfused tissues compartment before partitioning into the blood stream. Both of these methods

are less physiologically accurate as this compartment is a lumped entity comprised of various tissues throughout the body rather than in a single location (*e.g.*, liver); therefore, in the model described herein, the compound enters the bloodstream prior to reaching equilibrium in this diffuse tissue.

Craigmill (2003) and Yang et al. (2012) utilized similar stand-alone injection site compartments for intramuscular administration models in sheep and pigs, respectively. The sizes of these compartments were fixed at a set volume (0.5 or 1 kg, respectively) over which the volume of an injection is equilibrated prior to diffusion into the blood compartment. With the varied dose sizes used in the TMB-4 studies simulated here, utilizing a fixed volume method still has the dose being injected into a relatively large compartment, and results in a diluted dose absorbing into the blood stream. This could require re-adjusting parameters governing uptake into the blood whenever the size of the dose changes significantly. By using a volume for the IM compartment that is determined by the size of the dose, the concentration being absorbed into the blood stream will be more consistent for varying doses and should require fewer adjustments to the uptake parameters. Thus, the IM compartment used in this PBPK model has the advantage of adapting to real-world administration routes (the IM

compartment is created only when the intramuscular route is utilized), injection rates, and dosing volumes, potentially without having to adjust the fit PIM value between same-species studies.

Metabolism is included in model, contrary to the conclusions reached by Garrigue et al. (1991), the study on which this model was built. Garrigue and colleagues utilized chromatography to determine that no metabolites of TMB-4 were present in rat urine; however, their data indicated incomplete excretion of TMB-4 at 72 h, long after the oxime had left the blood. Metabolism of TMB-4 had been documented in rats, with de Miranda et al. (1972) first identifying the minor metabolite, trimethylene-1-(4-aldoximinopyridinium)-1'-(4-cyanopyridinium) ion (TACN) and Morgan et al. (1982) identifying the metabolite, trimethylene-1-(4-aldoximinopyridinium)-1'-(4-carbox-amidopyridinium) ion (TACARB) in rat urine. For the Garrigue et al. (1991) data, the TMB-4 PBPK model could not replicate the blood, tissue and urine data without metabolism to eliminate some of the TMB-4. The model simulations were visually fit to the Garrigue data set using an estimated 15 % metabolism over 72 h.

The model structure also incorporates saturable urinary clearance using the Michaelis–Menten equation to describe TMB-4 elimination. First-order urinary clearance does not adequately describe the rapid excretion of TMB-4, suggesting a potentially different mechanism of uptake in addition to absorption in the renal tubules (Sidell and Groff 1971; Swartz and Sidell 1974). Kayouka et al. (2011) have found that decreasing organic cation transport in rats, through competitive pretreatment with the organic cation tetraethylammonium or in knockout mice deficient in OCTs 1 and 2, resulted in significantly slower excretion of the oxime 2-PAM. Located primarily in proximal tubule cells, OCT transport from the blood across the basolateral membrane is dependent on a negative intracellular electrical gradient (Shu 2011), thereby rendering this transport saturable and subject to competitive interaction from other cationic drugs (Choi and Song 2008; Zhang et al. 1998).

Diffusion-limited uptake is utilized in all tissues and requires a tissue/blood PC and diffusion limitation coefficient constants (PA values) for each compartment. Fitting the data from Garrigue et al. (1991) requires larger tissue/blood PCs for kidney, liver and the slowly perfused tissue compartment (100.0, 12.0 and 10.0, respectively) than those predicted by QSPR, which predicted uptake to be similar across these tissues (Table 1), based on the organ lipid and water contents. Preferential uptake of oximes has been seen in rat liver and kidney by previous investigators (Lundy et al. 1990). Differences between predicted and fit PC values are thought to be the result of PC predictions not accounting for uptake limitation by active transport efflux mechanisms (Schmitt 2008), in addition to possible effects of tissue and/or blood binding (see *Species Differences*

below). The model is also unable to simulate the data with the predicted brain/blood PC of 0.91 in rats. Decreasing the PC to 0.13 is not unreasonable due to transporter-limited diffusion across the blood–brain barrier (BBB). Oximes are substrates for the active P-glycoprotein efflux transporter located in the BBB and do not easily enter the brain (Joosen et al. 2011). The model simulation of the Garrigue et al. (1991) study indicates that the maximum concentration in the plasma is nearly 18 times that in the brain (Fig. 3a, c); therefore, the necessity of the lower blood/brain PC was evident during model parameterization in order to simply simulate the efflux of the oxime through the BBB.

The model also requires small PA values, indicative of slow entry of TMB-4 into tissues. Although very water soluble, the charge and large size of TMB-4 molecules could slow their movement into tissues. The brain compartment requires the smallest PA value, necessary to simulate the influence of the blood–brain barrier on TMB-4 kinetics.

### Species differences

The TMB-4 PBPK model proves useful in highlighting differences in species' kinetics for this and potentially other oximes. The rat parameterization of this model requires kidney/blood, liver/blood and slowly perfused tissue/blood PCs much higher than those predicted by QSPR, while the brain/blood PC needs to be much lower. Without the fit PCs, the model cannot attain the relatively high concentrations of TMB-4 in the liver and kidney nor the very low concentrations of TMB-4 in the brain seen in data from Garrigue et al. (1991). The ability of the model to reasonably predict mouse data from Milic et al. (1996) while only fitting the length of intravenous injection (TInf) indicates that the kinetics in rodents are potentially similar. Human data, however, cannot be simulated utilizing these adjusted PCs. For the human parameterization, kidney/blood, liver/blood and slowly perfused tissue/blood PCs are adjusted back down to the QSPR-predicted values. This change accomplished satisfactory simulations and predictions to human blood and urine data, as human tissue data are not attainable. Potential sources of what may be significant kinetic differences between rodents and humans are explored below.

Garrigue et al. (1991) remarked on the high affinity of the oximes they tested, including TMB-4, for kidney, liver, cartilage and intervertebral discs in the rat. A year later, Garrigue and other colleagues (Maurizis et al. 1992) published an in vitro binding study of TMB-4 with rabbit cartilaginous tissue cultures. This study resulted in TMB-4 ionic binding not with the chondrocytes and fibroblasts themselves, but with the proteoglycans produced by these structures. Thus, the Maurizis et al. (1992) study may

explain, in part, the necessity of assuming an increased TMB-4 affinity for slowly perfused tissues, which include cartilage and similar structures, expressed in the model as a high tissue/blood PC. No data were available for determining whether human cartilage exhibits these same kinetics.

The affinity of TMB-4 for rat kidney and liver seen in the Garrigue et al. (1991) study may be due, at least in part, to the affinity of oximes for OCTs, which are expressed in both liver and kidney (Dresser et al. 2000) with kinetics and selectivity for particular organic cations differing between species. Dresser et al. (2000) especially noted differences in organic cation uptake affinity and kinetics between *Xenopus laevis* oocytes expressing human OCT 1 versus oocytes expressing rat or mouse OCT 1. Species-specific affinity for this and other OCTs could contribute to the need for significantly different liver and kidney tissue/blood PCs when switching from rodents to humans.

A literature search for blood-binding information with TMB-4 was unproductive. A search for blood binding with MMB-4 also failed to net articles. Binding research results for other oximes indicate potential species differences. 2-PAM has been shown, in vitro, to be bound 49 to 67 % with sheep plasma proteins (Srivastava and Malik 1988) and 64.7 % with goat plasma proteins (Rahal and Malik 2011); however, 2-PAM binding was not observed in vitro in human plasma or rat brain homogenate (Firemark et al. 1964). Ionic binding with a negatively charged structure is theoretically possible for any oxime, leaving potential binding as a research gap for individual oximes.

No attempt was made to alter the brain/blood PC in humans from the small value which had been fit to available rat brain data, although the other fit PCs from the rat model were not utilized in the human parameterization (i.e., liver, kidney and slowly perfused tissues/blood PCs) due to assumed species differences. The homology of the rat and human blood–brain barrier to TMB-4 is not specifically known; however, drug efficacy limitations due to P-glycoprotein and other efflux transporters in the BBB are well studied in both humans and rats. Blocking these membrane efflux transporters has been shown to improve brain drug concentrations in studies utilizing rats as the animal model (Joosen et al. 2011; Miller et al. 2008). In the absence of human brain data, the assumption was made that the fit value for the rat blood/brain PC is similar enough to the human blood/brain PC. Overall, model predictions for three species indicate a structure capable of interspecies extrapolation of TMB-4 kinetics.

#### Monte Carlo analyses

Following initial verification of the human model parameterization, MC analyses were conducted due to the poor

prediction for one of the two human evaluation data sets. The model is successful in predicting the lower dose of the intramuscular data from Calesnick and Christensen (1967), but significantly under-predicts the higher dose. It is unclear from the methods published in Calesnick and Christensen (1967) whether more than one volunteer was used at each dose level. It is entirely possible that the volunteer used for the upper dose was physiologically different than the lower-dose individual or the mid-range bodyweight and physiological parameters utilized for the model predictions. MC analyses were used to look at variability of all physiological parameters, since the use of male and female volunteers with the range in age and bodyweight described in the study indicate a physiologically diverse group. Following the MC analyses, the high-dose data are shown to fall within two SD of the human variability likely seen within this study. Use of MC analyses proved insightful, demonstrating that variation in physiological and physicochemical parameters between individuals impacts the model predictions and is found to be consistent with the TMB-4 blood clearances seen in the Calesnick and Christensen (1967) high-dose data.

#### Sensitivity analyses

As a final step in building this model, sensitivity analyses were run. Sensitivity analyses help characterize how well the model reflects the system in question; the parameters to which the model is sensitive should make sense physiologically and kinetically (Loizou et al. 2008). The analyses begin with the choice of critical endpoints, in this case TMB-4 concentrations in blood and brain. TMB-4 is eliminated very quickly, which reduces its efficacy in reactivating OP-inhibited AChE (Kayouka et al. 2011). A 3-h time course was chosen to capture the portion of the concentration curve most likely to be efficacious in an OP CWNA attack. Most oximes have a half-life of only 1–2 h (Voicu et al. 2010). The blood concentration endpoint provides a measure of TMB-4 being delivered to OP-inhibited AChE in the tissues. Reactivation of brain AChE, specifically in the ponto-medullary area, is paramount to survival following an OP exposure (Voicu et al. 2010), making the brain concentration of TMB-4 the other critical endpoint of choice.

All physiological, physicochemical and route-specific parameters for both intravenous and intramuscular routes were varied in the sensitivity analysis. Only two parameters were shown to result in model sensitivity across endpoints for both routes of administration: volume of venous blood (VVC) and volume of the slowly perfused tissue compartment (VSC). Both parameters are taken from published physiological values (Table 2). The model is sensitive to VVC only during the first few minutes of either exposure route. The model assumes instant mixing once the TMB-4

enters the blood from either the intravenous syringe or the IM compartment; small changes in the VVC result in relatively large changes in concentration in the blood and therefore in the brain. VSC represents the largest collective tissue volume of the body (62.7 % of body weight, Table 4), which greatly affects distribution of the water-soluble TMB-4. Although neither of these physiological values was altered in fitting the TMB-4 model, the tissue/blood partition coefficient for the slowly perfused tissue compartment, PS, was found to be critical in fitting the rat and human parameterizations of the model. The sensitivity of the model output to the slowly perfused tissue compartment in general indicates that the sheer size of this compartment and the TMB-4 that diffuses into it determines what's left over for the rest of the tissues in the model, blood and brain included.

An analysis of sensitivity is not complete without a look at the uncertainty of the parameters to which the endpoints are sensitive. The model was sensitive to several physiological parameters; specifically, the model was sensitive to VVC and VSC across administration routes and endpoints. Yet, these parameters are based on physiological measurement, reducing their uncertainty. Other physiological parameters would also be considered to have a low degree of uncertainty; however, physicochemical parameters used in this model, such as maximum rate constants and tissue/blood PCs, are more uncertain because they are either fit or predicted utilizing QSPR algorithms. While all PCs used in the model would be considered to have a relatively higher degree of uncertainty, the model was found to be sensitive to only the brain/blood PC (PBr), the IM compartment tissue/blood PC (PIM) and the kidney/blood PC (PK). Other uncertain physicochemical parameters to which the model is sensitive include the blood/brain diffusion limitation coefficient (PABrC) and the excretion parameters (maximum saturable excretion rate constant (VMaxUrC) and excretion affinity constant (KmUr)). Additional laboratory studies designed to measure even a few of these parameters would reduce the overall uncertainty in the model.

#### Model application and future work

The purpose of this TMB-4 model is to act as a stepping stone for prediction of MMB-4 kinetics. Unfortunately, published MMB-4 pharmacokinetic data were not found for any of the three species for which this model was developed. However, with consideration for the assumptions made, the model can predict anticipated MMB-4 kinetics in humans. Figure 12 depicts the simulated Vojvodic (1970) TMB-4 study kinetics from Fig. 6a along with predicted kinetics of an equimolar MMB-4 dose given under identical conditions. Aside from the lower molecular weight of MMB-4 compared to TMB-4 (258.27 vs.

286.33 g/mol), only predicted tissue/blood PC values changed between model parameterizations (Table 6). Fit tissue/blood PC values (PBr and PIM) and tissue permeability area cross products remained the same as in the TMB-4 parameterization. The model predicts a slightly lower concentration of MMB-4 as compared to the equimolar dose of TMB-4, due to the lesser molecular weight of MMB-4. Since the predicted pharmacokinetics of these oximes are very similar, the improved equimolar efficacy of MMB-4 over TMB-4 (Shih et al. 2009) is likely a pharmacodynamic difference.

A key strength of PBPK models is that they can be utilized to predict human blood levels of a drug over a variety of dosing regimens. Following the comparison made in Fig. 12, the model was utilized to predict a presumably efficacious dose in humans under a dosing regimen consistent with military deployment (Fig. 13). Under the current protocol, soldiers are issued three MARK I kits (Newmark 2009) and are instructed to self- or buddy-administer one kit immediately at the first signs of nerve agent poisoning. Up to 2 more kits may be administered every 10–15 min if symptoms persist (USAF 1996). Proper use of autoinjectors involves holding the unit in place for 10 s to ensure complete transfer of the drug to the patient (CHEMM 2011). Using these administration guidelines, the model was iteratively run using progressive doses until a presumably efficacious blood concentration lasting more than 2 hours was achieved. In vitro data from Worek et al. (2010) indicate that human erythrocytes with AChE levels inhibited in excess of 95 % by sarin, cyclosarin, VX or VR may be reactivated to 40 % AChE activity by a media concentration of 50  $\mu$ M MMB-4, theoretically equivalent to a blood concentration of 12.9 mg MMB-4 cation/L. The model predicts that 3 autoinjectors, each containing the equivalent of 5 mg MMB-4/kg, would result in a potentially efficacious dose lasting more than 2 h in a 70 kg person. This scenario assumes that the soldier would receive medical assistance beyond buddy care before the 3-h mark; additional autoinjectors would be needed to maintain an efficacious dose beyond that time point if medical care did not arrive. A significant concern with this scenario is the length of time necessary for the blood concentration to reach the efficacy level (21 min), providing the soldier received a CWNA dose high enough to result in more than 95 % inhibition of AChE. Administering all three autoinjectors one after the other brings the time to efficacy down to 9.24 min, assuming autoinjectors were given 40 s apart to allow time for proper package handling (simulation not shown). These model predictions do raise concern that the current method of administering oximes in the field may not result in an efficacious blood concentration rapidly enough to save the lives of those exposed to high levels of CWNAs.

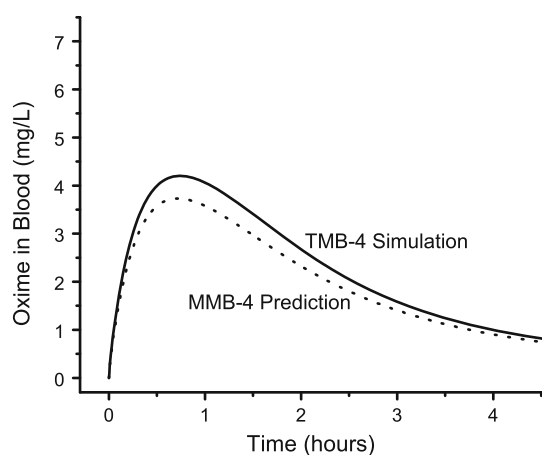


**Fig. 12** Comparison of TMB-4 model simulation of Vojvodic (1970) study protocol (solid line, see Fig. 6) and prediction of an equimolar MMB-4 dose (dotted line). Model conditions were set for a 81.9 kg male human receiving either 2.45 mg TMB-4/kg BW or 2.21 mg MMB-4/kg BW, dosed intramuscularly

**Table 6** Tissue/blood partition coefficients used in the MMB-4 and TMB-4 model parameterizations for humans

Tissue/blood partition coefficients (unitless) <sup>a</sup>		MMB-4	TMB-4 <sup>b</sup>
Brain	PBr	0.13*	0.13 <sup>#</sup>
Diaphragm	PD	0.94	0.94
Fat	PF	0.24	0.19
IM compartment	PIM	2.5*	2.5 <sup>#</sup>
Kidney	PK	0.94	0.94
Liver	PL	0.90	0.90
Rapidly perfused	PR	0.98	0.97
Slowly perfused	PS	0.74	0.74

<sup>a</sup> PC values predicted unless otherwise noted; <sup>b</sup> Values from Table 3

\* Value from TMB-4 model; <sup>#</sup>Fit value

Although the model can be used in its present state to help predict MMB-4 kinetics, further development and model validation is recommended utilizing MMB-4 kinetic data. Since rats are considered poor animal models of CWNA effects due to the abundance of carboxylesterase in rat blood and its bioscavenging activity against OP compounds (Maxwell and Brecht 2001), further model development for oximes as OP reactivators should be pursued in another species, such as the guinea pig. Therefore, guinea pig blood, liver, kidney, brain and urine time course kinetics of MMB-4 would provide a solid basis for further model development. Additionally, blood, urine and tissue kinetics in non-human primates would allow some insight into the magnitude of species differences in tissue/blood PCs, metabolism and urinary excretion highlighted in the current phase of the model. Blood and urine kinetics for

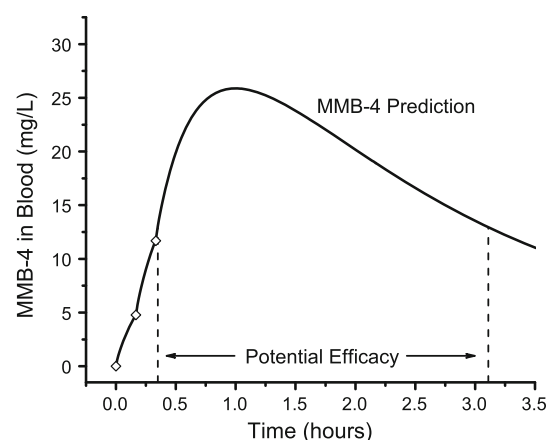


**Fig. 13** Prediction (line) of presumably efficacious dose of MMB-4 for military use. Model conditions were set for a 70 kg human administered 3 autoinjectors 10 min apart containing the equivalent of 5 mg MMB-4/kg. Open diamonds indicate successive doses while the dotted lines indicate the period of time over which the blood concentration exceeded the potential efficacious level of 12.9 mg/L per in vitro data by Worek et al. (2010)

MMB-4 in human volunteers would help support species extrapolation assumptions.

While the MMB-4 parameterization of the model is still awaiting further development should the opportunity arise in the form of newly available kinetic data, the TMB-4 PBPK model parameterization can now be expanded to incorporate pharmacodynamic effects, including oxime reactivation of OP-AChE complexes, to better extrapolate efficacy across the human population under different dosing regimens. The resulting PBPK-pharmacodynamic mathematical model would allow in silico testing of countermeasure dosing regimens and facilitate extrapolation of novel oxime effects in experimental animals to humans, thereby optimizing therapeutic efficacy.

**Acknowledgments** This project received support from the Defense Threat Reduction Agency-Joint Science and Technology Office, Basic and Supporting Sciences Division (1.E0056.08.AHB.C).

**Conflict of interest** The authors declare that they have no conflict of interest.

## References

- Arms AD, Travis CC (1988) Reference physiological parameters in pharmacokinetic modeling. U.S. Environmental Protection Agency, Office of Health and Environmental Assessment, Washington, DC, EPA/600/6-88/004, NTIS PB88-196019
- Bosse JA, Wassermann O (1970) On the blood content of guinea-pig tissues. *Pharmacology* 4:273–277
- Brown RP, Delp MD, Lindstedt SL, Rhomberg LR, Beliles RP (1997) Physiological parameter values for physiologically based pharmacokinetic models. *Toxicol Ind Health* 13:407–484

- Calesnick B, Christensen RM (1967) Human toxicity of various oximes. 2-Pyridine aldoxime methyl chloride, its methane sulfonate salt, and 1,1'-trimethylenebis-(4-formylpyridinium chloride). *Arch Environ Health* 15:599–608
- CHEMM (2011) Nerve agent treatment—autoinjector instructions. U.S. Department of Health and Human Services, Chemical Hazards Emergency Medical Management, Washington, DC. Updated 25 Jun 2011. Accessed 9 Aug 2012. [http://chemm.nlm.nih.gov/antidote\\_nerveagents.htm](http://chemm.nlm.nih.gov/antidote_nerveagents.htm)
- Chen K, Seng KY (2012) Calibration and validation of a physiologically based model for Soman intoxication in the rat, marmoset, guinea pig and pig. *J Appl Toxicol* 32(9):673–686
- Choi MK, Song IS (2008) Organic cation transporters and their pharmacokinetic and pharmacodynamic consequences. *Drug Metab Pharmacokinet* 23:243–253
- Clewell HJ, Gentry PR, Gearhart JM, Allen BC, Andersen ME (2001) Comparison of cancer risk estimates for vinyl chloride using animal and human data with a PBPK model. *Sci Total Environ* 274:37–66
- Copp SW, Hageman KS, Behnke BJ, Poole DC, Musch TI (2010) Effects of Type II diabetes on exercising skeletal muscle blood flow in the rat. *J Appl Physiol* 109:1347–1353
- Covington TR, Robinan GP, Van Landingham CB, Andersen ME, Kester JE, Clewell HJ (2007) The use of Markov chain Monte Carlo uncertainty analysis to support a public health goal for perchloroethylene. *Regul Toxicol Pharmacol* 47:1–18
- Craigmill AL (2003) A physiologically based pharmacokinetic model for oxytetracycline residues in sheep. *J Vet Pharmacol Therap* 26(1):55–63
- Davies B, Morris T (1993) Physiological parameters in laboratory animals and humans. *Pharm Res* 10:1093–1095
- de Miranda P, Feitknecht UF, Gibbon SL, Burrows GE, Way JL (1972) Urinary metabolite of 1,1'-trimethylene-bis (4-aldoximinopyridinium) dibromide (TMB-4) in the rat. I. Trimethylene-1-(4-aldoximinopyridinium)-1'-(4-cyanopyridinium) dibromide. *J Pharmacol Exp Ther* 180:435–445
- Dresser MJ, Gray AT, Giacomini KM (2000) Kinetic and selectivity differences between rodent, rabbit, and human organic cation transporters (OCT1). *J Pharmacol Exp Ther* 292(3):1146–1152
- Eddleston M, Buckley NA, Eyer P, Dawson AH (2008) Management of acute organophosphorus pesticide poisoning. *Lancet* 371:597–607
- Eyer P (2003) The role of oximes in the management of organophosphorus pesticide poisoning. *Toxicol Rev* 22:165–190
- Eyer PA, Worek F (2007) Oximes. In: Marrs TC, Maynard RL, Sidell FR (eds) *Chemical warfare agents toxicology and treatment*, 2nd edn. Wiley, West Sussex, pp 305–329
- Firemark H, Barlow CF, Roth LJ (1964) The penetration of 2-PAM-C14 into brain and the effect of cholinesterase inhibitors on its transport. *J Pharmacol Exp Ther* 145:252–265
- Garrigue H, Maurizis JC, Madelmont JC, Nicolas C, Meyniel JM, Louvel A, Demerseman P, Sentenac-Roumanou H, Veyre A (1991) Disposition and metabolism of acetylcholinesterase reactivators 2PAM-I, TMB4 and R665 in rats submitted to organophosphate poisoning. *Xenobiotica* 21:583–595
- Gearhart JM, Jepson GW, Clewell HJ, Andersen ME, Conolly RB (1990) Physiologically based pharmacokinetic and pharmacodynamic model for the inhibition of acetylcholinesterase by diisopropylfluorophosphate. *Toxicol Appl Pharmacol* 106:295–310
- Gearhart JM, Jepson GW, Clewell HJ, Andersen ME, Conolly RB (1994) Physiologically based pharmacokinetic model for the inhibition of acetylcholinesterase by organophosphate esters. *Environ Health Perspect* 102(suppl 11):51–60
- Joosen MJ, van der Schans MJ, van Dijk CG, Kuijpers WC, Wortelboer HM, van Helden HP (2011) Increasing oxime efficacy by blood-brain barrier modulation. *Toxicol Lett* 206:67–71
- Kayouka M, Houze P, Baud FJ, Cisternino S, Debray M, Risede P, Schinkel AH, Warnet JM (2011) Does modulation of organic cation transporters improve pralidoxime activity in an animal model of organophosphate poisoning? *Crit Care Med* 39:803–811
- Kohn MC (2002) Use of sensitivity analysis to assess reliability of metabolic and physiological models. *Risk Anal* 22:623–631
- Koplovitz I, Schulz SM, Railer RF, Sigler M, Lee RB (2007) Effect of atropine and diazepam on the efficacy of oxime treatment of nerve agent intoxication. *J Med CBR Def* 5:1–15
- Kovarik Z, Calic M, Sinko G, Bosak A (2007) Structure-activity approach in the reactivation of tabun-phosphorylated human acetylcholinesterase with bispyridinium para-aldoximes. *Arh Hig Rada Toksikol* 58:201–209
- Loizou G, Spendiff M, Barton HA, Bessems J, Bois FY, d'Yvoire MB, Buist H, Clewell HJ, Meek B, Gundert-Remy U, Goerlitz G, Schmitt W (2008) Development of good modelling practice for physiologically based pharmacokinetic models for use in risk assessment: the first steps. *Regul Toxicol Pharmacol* 50:400–411
- Lundy PM, Hand BT, Broxup BR, Yipchuck G, Hamilton MG (1990) Distribution of the bispyridinium oxime 14C HI-6 in male and female rats. *Arch Toxicol* 64:377–382
- Lundy PM, Hamilton MG, Sawyer TW, Mikler J (2011) Comparative protective effects of HI-6 and MMB-4 against organophosphorus nerve agent poisoning. *Toxicology* 285:90–96
- Maurizis JC, Ollier M, Nicolas C, Madelmont JC, Garrigue H, Veyre A (1992) In vitro binding of oxime acetylcholinesterase reactivators to proteoglycans synthesized by cultured chondrocytes and fibroblasts. *Biochem Pharmacol* 44:1927–1933
- Maxwell DM, Brecht KM (2001) Carboxylesterase: specificity and spontaneous reactivation of an endogenous scavenger for organophosphorus compounds. *J Appl Toxicol* 21(suppl 1):S103–S107
- Milic B, Maksimovic M, Nedeljkovic M (1996) Trimedoxime and HI-6: kinetic comparison after intravenous administration to mice. *Pharmacol Toxicol* 78:269–272
- Miller DS, Bauer B, Hartz AM (2008) Modulation of P-glycoprotein at the blood-brain barrier: opportunities to improve central nervous system pharmacotherapy. *Pharmacol Rev* 60(2):196–209
- Morgan RL, Burrows GE, Yen MH, Way JL (1982) Metabolic disposition of the alkylphosphate antagonist, 1,1'-trimethylenebis(4-aldoximinopyridinium) ion (TMB-4), in the rat. III. Trimethylene-1-(4-aldoximinopyridinium)-1'-(4-carboxamidopyridinium) ion. *Drug Metab Dispos* 10:491–494
- Newmark J (2009) Nerve agents. In: Dobb MR (ed) *Clinical neurotoxicology: syndromes, substances, environments*. Saunders Elsevier, Philadelphia, PA, pp 646–659
- Office of the Campus Veterinarian (OCV) (2011) Guidelines for handling, restraint, injections and blood collection from small laboratory animals. Washington State University, Pullman WA. <http://campusvet.wsu.edu/infocac/handling.htm>. Accessed 3 Aug 2011
- Rahal A, Malik JK (2011) Pharmacokinetics, urinary excretion and plasma protein binding of pralidoxime in goats. *Sm Rumin Res* 95:179–183
- Saxena A, Luo C, Chilukuri N, Maxwell DM, Doctor BP (2008) Novel approaches to medical protection against chemical warfare nerve agents. In: Romano JA, Lukey BJ, Salem H (eds) *Chemical warfare agents: chemistry, pharmacology, toxicology and therapeutics*. CRC Press, New York, pp 145–173
- Schmitt W (2008) General approach for the calculation of tissue to plasma partition coefficients. *Toxicol In Vitro* 22:457–467
- Shih TM, Skovira JW, O'Donnell JC, McDonough JH (2009) Evaluation of nine oximes on in vivo reactivation of blood,

- brain, and tissue cholinesterase activity inhibited by organophosphorus nerve agents at lethal dose. *Toxicol Mech Methods* 19:386–400
- Shu Y (2011) Research progress in the organic cation transporters. *Zhong Nan Da Xue Xue Bao Yi Xue Ban* 36(10):913–926
- Sidell FR, Groff WA (1971) Intramuscular and intravenous administration of small doses of 2-pyridinium aldoxime methochloride to man. *J Pharm Sci* 60:1224–1228
- Srivastava AK, Malik JK (1988) Biodistribution and plasma protein binding of 2-formyl-1-methyl pyridinium methiodide (2-PAM) in sheep (*Ovis aries*). *Indian J Exp Biol* 26:643–644
- Stemler FW, Tezak-Reid TM, McCluskey MP, Kaminskis A, Corcoran KD, Shih ML, Stewart JR, Wade JV, Hayward IJ (1991) Pharmacokinetics and pharmacodynamics of oximes in unanesthetized pigs. *Fundam Appl Toxicol* 16:548–558
- Swartz RD, Sidell FR (1974) Renal tubular secretion of pralidoxime in man. *Proc Soc Exp Biol Med* 146:419–424
- USAF (1996) Self aid and buddy care instructor handbook. Air Force Handbook 36-2218, vol 1. United States Air Force, Washington, DC. <http://www.e-publishing.af.mil/shared/media/epubs/AFH36-2218V1.pdf>
- Voicu VA, Bajgar J, Medvedovici A, Radulescu FS, Miron DS (2010) Pharmacokinetics and pharmacodynamics of some oximes and associated therapeutic consequences: a critical review. *J Appl Toxicol* 30:719–729
- Vojvodic VB (1970) Blood levels, urinary excretion and potential toxicity of N, N'-trimethylethylbis (pyridinium-4-aldoxime) dichloride (TMB-4) in healthy man following intramuscular injection of the oxime. *Pharmacol Clin* 2:216–220
- Worek F, Szinicz L, Eyer P, Thiermann H (2005) Evaluation of oxime efficacy in nerve agent poisoning: development of a kinetic-based dynamic model. *Toxicol Appl Pharmacol* 209:193–202
- Worek F, Wille T, Aurbek N, Eyer P, Thiermann H (2010) Reactivation of organophosphate-inhibited human, *Cynomolgus* monkey, swine and guinea pig acetylcholinesterase by MMB-4: a modified kinetic approach. *Toxicol Appl Pharmacol* 249(3):231–237
- Wu AHB (2006) Tietz clinical guide to laboratory tests, 4th edn. Saunders Elsevier, St. Louis, MO
- Yang F, Liu HW, Li M, Ding HZ, Huang XH, Zeng ZL (2012) Use of a Monte Carlo analysis within a physiologically based pharmacokinetic model to predict doxycycline residue withdrawal time in edible tissues in swine. *Food Addit Contam Part A Chem Anal Control Expo Risk Assess* 29(1):73–84
- Zhang L, Brett CM, Giacomini KM (1998) Role of organic cation transporters in drug absorption and elimination. *Annu Rev Pharmacol Toxicol* 38:431–460
- Zhao P, Zhang L, Grillo JA, Liu Q, Bullock JM, Moon YJ, Song P, Brar SS, Madabushi R, Wu TC, Booth BP, Rahman NA, Reynolds KS, Gil BE, Lesko LJ, Huang SM (2011) Applications of physiologically based pharmacokinetic (PBPK) modeling and simulation during regulatory review. *Clin Pharmacol Ther* 89:259–267

